UNCLASSIFIED

AD NUMBER

AD915601

NEW LIMITATION CHANGE

TO

Approved for public release, distribution unlimited

FROM

Distribution authorized to U.S. Gov't. agencies only; Test and Evaluation; AUG 1973. Other requests shall be referred to Air Force Armament Laboratory, Attn: DLYA, Eglin AFB, FL 32542.

AUTHORITY

AFATL ltr, 6 Jun 1977

THIS PAGE IS UNCLASSIFIED

AD915601

AFATL-TR-73-160
VOLUME I

CALCULATION OF SHAPED-CHARGE JETS USING ENGINEERING APPROXIMATIONS AND FINITE DIFFERENCE COMPUTER CODES

VOLUME I. GENERALIZED ANALYTICAL APPROACH TO SHAPED-CHARGE WARHEAD DESIGN

PHYSICS INTERNATIONAL COMPANY

DDC
RECEIVED
DEC 19 1973
B

TECHNICAL REPORT AFATL-TR-73-160, VOLUME I

AUGUST 1973

Distribution limited to U. S. Government agencies only; this report documents test and evaluation; distribution limitation applied August 1973 . Other requests for this document must be referred to the Air Force Armament Laboratory (DLYA), Eglin Air Force Base, Florida 32542.

AIR FORCE ARMAMENT LABORATORY

AIR FORCE SYSTEMS COMMAND • UNITED STATES AIR FORCE

EGLIN AIR FORCE BASE, FLORIDA

Calculation Of Shaped-Charge Jets Using Engineering Approximations And Finite Difference Computer Codes

Volume I. Generalized Analytical Approach To Shaped-Charge Warhead Design

L. Behrmann

Distribution limited to U. S. Government agencies only; this report documents test and evaluation; distribution limitation applied August 1973 . Other requests for this document must be referred to the Air Force Armament Laboratory (DLYA), Eglin Air Force Base, Florida 32542.

FOREWORD

This report was prepared by Physics International Company, 2700 Merced Street, San Leandro, California 94577, under Contract No. F08635-72-C-0229 with the Air Force Armament Laboratory, Eglin Air Force Base, Florida. Mr. Lovonia J. Theriot (DLYA) managed the program for the Armament Laboratory. This effort was conducted during the period from June 1972 to April 1973.

The contractor report number assigned is PIFR-430.

This report is divided into two volumes. Volume I presents the generalized analytical approach to shaped-charge warhead design. Volume II describes the modification and utilization of a two-dimensional finite difference continuum mechanics code utilizing the Lagrangian coordinate system to calculate the complete jet formation parameters for any generalized axisymmetric shaped charge. This is Volume I.

This technical report has been reviewed and is approved.

Robert W. Dillon

ROBERT W. DILLON, Colonel, USAF
Chief, Weapons Systems Analysis Division

ABSTRACT

This report describes a technique to optimize the current shaped-charge design procedure as follows. Starting with the desired target to be defeated, a determination of the desired penetration characteristics of the jet would be made. Existing jet penetration theory would then be used to estimate the ideal characteristics of the jet to defeat the given target. A shaped-charge launcher would then be designed to give these ideal jet characteristics. However, a suitable design procedure requires (1) a viable analytical or empirical design approach to obtain a first cut shaped charge design, (2) a better understanding than now exists of the detailed mechanisms of jet formation, and (3) a better understanding of the phenomenon of jet penetration. This report, which is contained in two volumes, addresses the first two of these requirements. Volume I describes the use of the existing non-steady state theory of jet formation with experimental data and one-dimensional finite difference continue mechanics calculations to obtain the liner collapse velocity for generalized axisymmetric shaped charges. The results of this work are then used to obtain nonunique shaped charge designs which give the required idealized jet parameters. Volume II describes the modification and utilization of a two-dimensional finite difference continuum mechanics code utilizing the Lagrangian Coordinate system to calculate the complete jet formation parameters for any generalized axisymmetric shaped charge. The utilization of this code allows a more detailed study of such phenomena as jet stability, bifurcation on the axis, shear gradients, viscosity, shocks, incipient vaporization, surface tension, and possible other effects. The combined use of both the engineering formulations along with the sophisticated two-dimensional code calculation allows design engineers the versatility to design the most optimum shaped charge for their particular application.

Distribution limited to U. S. Government agencies only; this report documents test and evaluation; distribution limitation applied August 1973 . Other requests for this document must be referred to the Air Force Armament Laboratory (DLYA), Eglin Air Force Base, Florida 32542.

(The reverse of this page is blank)

TABLE OF CONTENTS

Section		Page
I	INTRODUCTION	1
II	GENERALIZATION OF THE NONSTEADY THEORY OF JET FORMATION	3
	1. Derivation of Jet Parameters	3
	2. Examination of the Jet Parameter Technique	8
III	DETERMINATION OF LINER COLLAPSE VELOCITIES	14
	1. Approach	14
	2. Procedure	15
IV	APPLICATION OF THE JET PARAMETER EQUATIONS	32
	1. BRL 105 mm Precision Shaped Charge	32
	2. Design of a Near Constant Jet Velocity Shaped Charge	34
V	CONCLUSION	41
	REFERENCES	42

LIST OF FIGURES

Figure	Title	Page
1	Generalized Axisymmetric Shaped Charge Configuration	4
2	Variation of Jet/Liner Velocity Ratio with	10
3	Variation of β with V_o'/V_o	11
4	Variation of β with V_o	12
5	Variation of β with α'	13
6	105 mm Unconfined Test Charge	16
7	Collapse Velocity Versus Time at R = 1.535 cm (Zones 0 Through 3)	18
8	Collapse Velocity Versus Time at R = 1.535 cm (Zones 12 Through 15)	19
9	Collapse Velocity Versus Time at R = 2.25 cm (Zones 0 Through 3)	20
10	Collapse Velocity Versus Time at R = 2.25 cm (Zones 10 Through 15)	21
11	Collapse Velocity Versus Time at R = 2.82 cm at R = 2.82 cm (Zones 0 Through 3)	22
12	Collapse Velocity Versus Time at R = 2.82 cm at R = 2.82 cm (Zones 10 Through 15)	23
13	Collapse Velocity Versus Time at R = 3.21 cm at R = 3.21 cm (Zones 0 Through 3)	24
14	Collapse Velocity Versus Time at R = 3.21 cm at R = 3.21 cm (Zones 12 Through 15)	25

LIST OF FIGURES (Concluded)

Figure	Title	Page
15	Velocity Profile Through Liner Thickness at the Time of Collapse	26
16	Average Velocity Per Liner Increment at the Time of Collapse	28
17	Proposed Correlation Between Calculated and Semi-Empirical Steady State Collapse Velocities	29
18	Equivalent Steady State Collapse Velocity for Axisymmetric Imploded Liners	30
19	105 mm Precision Shaped Charge Warhead	33
20	Liner Collapse Velocity for the BRL 105 mm Precision Shaped Charge	35
21	Calculated Jet Parameters for the BRL 105 mm Precision Shaped Charge	36
22	Geometry for a Near Constant Jet Velocity Shaped Charge	38
23	Liner Collapse Velocity for Shaped Charge Geometry Shown in Figure 23	39
24	Jet Parameters for Shaped Charge Geometry Shown in Figure 23	40

(The reverse of this page is blank)

SECTION I

INTRODUCTION

Conical metallic-lined shaped charges have been in existence for 30 years and during this time the basic design has changed little. The qualitative theory of jet formation and jet penetration was first published in 1948 (Reference 1). This theory was based upon the classical hydrodynamic theory of perfect fluids and thus assumed steady state conditions to exist and required material flow with average properties which conserved mass, momentum, and energy. In order to partition the energy unequivocably, the authors had to ignore the role played by shocks in the acceleration of the conical liner. The theory presented in Reference 1 assumed that each element of the conical liner collapsed with a constant velocity and thus the resulting jet was one with uniform properties. Uniform properties imply that the jet mass per-unit length of jet and the jet velocity for each element of the jet were equal for the total length of the jet. The steady state theory of jet formation was modified in 1952 (Reference 2) to account for the variable liner collapse velocity. This nonsteady theory for jet formation was then re-examined in 1954 by Eichelberger (Reference 3) and has seen no further basic modifications since that time. Since 1954 the majority of the literature discussing jet parameters has been the correlation of extensive experimental data with the nonsteady jet formation theory to obtain empirically the liner collapse velocities. Once the liner collapse velocities were available for a given charge design and explosive, then quick calculations could be performed to determine the jet parameters from other explosive charges or scaled versions of the same design. However, if the charge-to-mass ratio (c/m) of the design of the liner angle or geometry were changed then additional experimental data was necessitated to obtain the collapse velocity as a function of liner element

for the new design. The missing link to the straightforward utilization of the jet formation theory, as given in Reference 3, is an equation or data that gives the collapse velocity of the liner as a function of the explosive charge and the radius of the liner from the axis of the shaped charge configuration. Analytical expressions for the collapse velocity of flat plates as a function of the above parameters have been investigated by several authors; two of the most recent are given in References 4 and 5. Similar analytical solutions to the problem of the implosion of infinite cylinders by explosive are not possible at this time. The basic reason for this is that the material at the inside of the cylindrical liner experiences an acceleration due to the convergent pressures, and thus the velocities through the liner thickness are highly nonuniform.

Existing experimental data on the collapse velocity of shaped charges plus one-dimensional calculations to simulate the collapse of a shaped-charge liner are used to develop a predictive capability of the collapse velocities of imploding cylinders as a function of c/m and distance of the liner from the impact axis. This empirical data, combined with the nonsteady state theory of jet formation, provides a convenient tool to design a shaped charge for given jet parameters. This design would then constitute an initial geometry configuration which could be fine tuned by the use of a two-dimensional finite difference calculation.

SECTION II

GENERALIZATION OF THE NONSTEADY THEORY OF JET FORMATION

1. DERIVATION OF JET PARAMETERS

The theory of jet formation as given in References 1 through 3 was restricted to a liner with a constant cone angle. To obtain the maximum flexibility in the design of a shaped charge to give desired jet parameters, it is desirable to allow a generalization in the liner thickness, geometric shape, and point of initiation.

From Reference 2, the important equations are:

$$\delta(x) = \sin^{-1} [V_o(x) \cos \varepsilon(x)/2\, U_D]; \tag{1}$$

$$V_j(x) = V_o(x) \cos [\alpha(x) + \delta(x) - \beta(x)/2]/\sin\beta(x)/2 \tag{2}$$

$$dm_j(x)/dm(x) = \sin^2 \beta(x)/2 \tag{3}$$

$$dm_s(x)/dm(x) = \cos^2 \beta(x)/2 \tag{4}$$

Referring to Figure 1, δ is the angle between the direction an element of the liner travels after being struck by the detonation wave and normal to the liner surface, V_o is the velocity at which the liner element travels toward the axis, and α is the angle between the tangent to the liner at a point x and the axis of the liner.

U_D is the detonation velocity of the explosive; V_j, the velocity of the jet element formed; β, the angle between the collapsing liner wall and the axis; ε is the angle between the

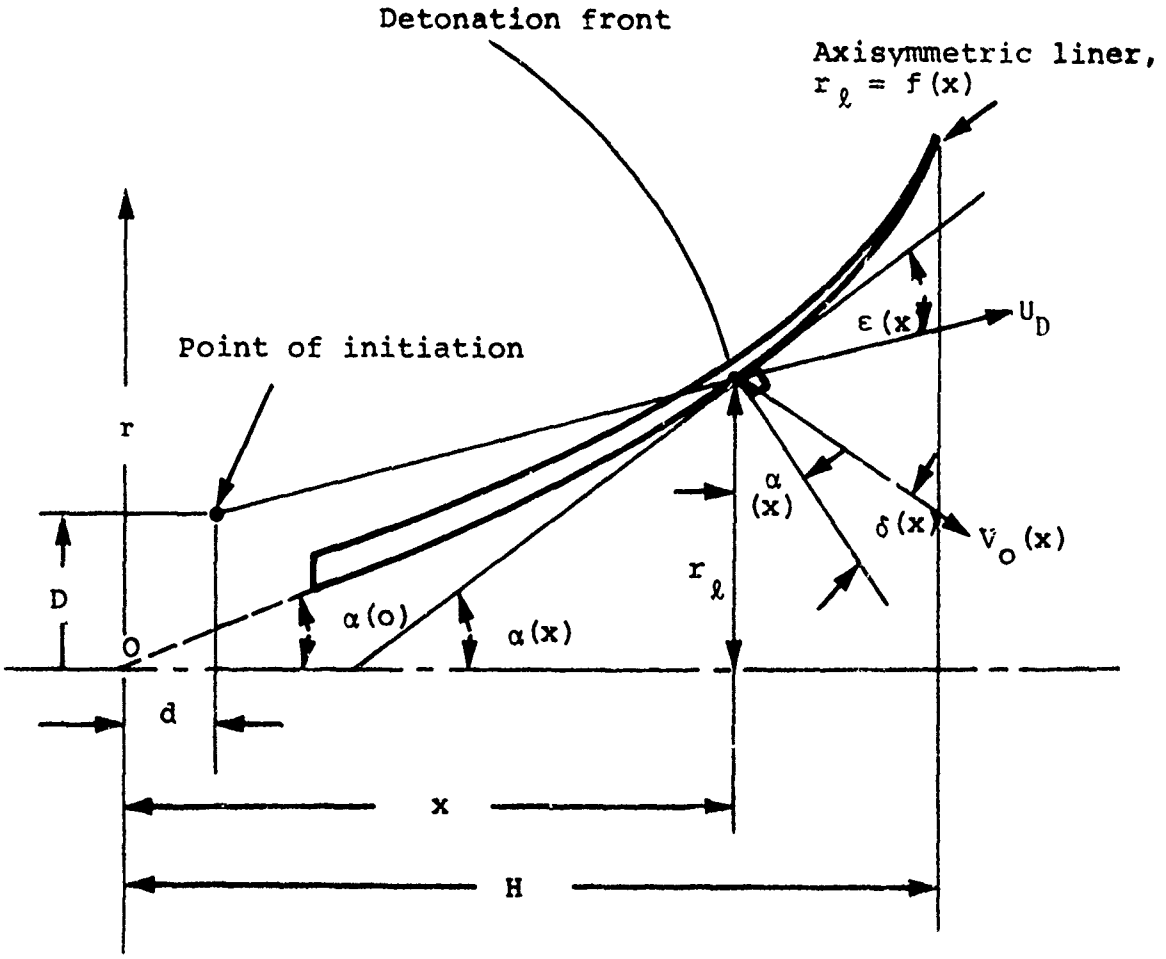

Figure 1. Generalized Axisymmetric Shaped-Charge Configuration

explosive detonation velocity vector and the tangent to the liner; m_s, the mass of the slug; m_j, the mass of the jet, and m, the mass of the liner. The masses m_s, m_j and m are each functions of x. The mass m is that part of the mass of the liner that is included between the top (apex) (x = 0) of the liner and the plane perpendicular to liner axis at x = x. The masses m_s and m_j are the parts of m that end up in the slug and the jet respectively.

As seen from Equations (1 through 4), once the collapse velocity V_o and the collapse angle β is determined, then the jet velocity V_j and jet mass dm_j can be obtained. Following the work of Reference 2, the collapse angle is obtained as a function of the liner geometry and collapse velocity.

From Figure 1, the following geometrical relations are developed:

$$\tan(\alpha - \varepsilon) = (r_\ell - D)/(x - d); \tag{5}$$

$$T(x) = \frac{1}{U_D}\left[\{x - d\}^2 + \{r_\ell(x) - D\}^2\right]^{\frac{1}{2}}; \tag{6}$$

$$r(x) = r_\ell(x) - V_o(x)\,[t(x) - T(x)]\cos[\alpha(x) + \delta(x)]; \tag{7}$$

$$Z(x) = X + V_o(x)\,[t(x) - T(x)]\sin\alpha[(x) + \delta(x)] \tag{8}$$

r_ℓ is the radius of the liner at a point x; T is the time the detonation front takes to reach a point x on the liner; t is the time it takes for a point x on the liner to reach a radius r, and z is the corresponding x coordinate. The tangent of the collapse angle, β, at any given time, t, is by definition the partial derivative of r with respect to z at constant t.

Therefore, we have from equations (7) and (8):

$$\left.\frac{\partial r}{\partial z}\right|_t = \left.\frac{\partial x}{\partial z}\right|_t \left[\frac{\partial r_\ell}{\partial x} - V_o t \frac{\partial \cos A}{\partial x} - \frac{\partial V_o}{\partial x} t \cos A + V_o \left\{T \frac{\partial \cos A}{\partial x} + \frac{\partial T}{\partial x} \cos A\right\} + \frac{\partial V_o}{\partial x} T \cos A\right]; \tag{9}$$

$$\left.\frac{\partial z}{\partial x}\right|_t = 1 + V_o t \frac{\partial \sin A}{\partial x} + \frac{\partial V_o}{\partial x} t \sin A - \frac{\partial V_o}{\partial x} T \sin A - V_o \left\{T \frac{\partial \sin A}{\partial x} + \frac{\partial T}{\partial x} \sin A\right\}; \tag{10}$$

where $A = \alpha + \delta$.

Using the following relations and rearranging equations (9) and (10), we have:

$$\frac{\partial}{\partial x} \cos A = - \sin A \, (\alpha' + \delta');$$

$$\frac{\partial}{\partial x} \sin A = \cos A \, (\alpha' + \delta');$$

where the prime indicates differentiation with respect to x,

$$\left.\frac{\partial r}{\partial z}\right|_t = \left.\frac{\partial x}{\partial z}\right|_t \left[\frac{\partial r_\ell}{\partial x} - (t - T) \left\{V_o' \cos A - V_o \, (\alpha'+\delta') \sin A\right\} + V_o T' \cos A\right]; \tag{11}$$

$$\left.\frac{\partial x}{\partial z}\right|_t = 1 + (t - T) \left\{V_o \, (\alpha'+\delta') \cos A + V_o' \sin A\right\} - V_o T' \sin A \tag{12}$$

The collapse angle of interest is at r = 0 when an element at the point x on the liner reaches the axis. Therefore from equation (7), the corresponding time at r = 0 is given as:

$$t - T = \frac{r_\ell}{V_o \cos A} \tag{13}$$

Substituting (13) into (11) and (12) and dividing (11) by (12) gives $\tan \beta = \partial r/\partial z \Big|_{r=0}$;

$$\tan \beta \Big|_{r=0} = \frac{\tan \alpha + r_\ell \left[(\alpha' + \delta') \tan A - V_o'/V_o \right] + V_o T' \cos A}{1 + r_\ell \left[(\alpha' + \delta') + V_o'/V_o \tan A \right] - V_o T' \sin A} \tag{14}$$

Therefore, once a liner geometry is chosen and the liner collapse velocities determined, the jet parameters can be calculated.

Before proceeding with the use of these equations, the equations to calculate δ', ε', and T' will be obtained.

From equation (1),

$$\sin \delta = V_o \cos \varepsilon / 2 U_D;$$

$$\delta' \cos \delta = \frac{V_o' \cos \varepsilon - V_o \varepsilon' \sin \varepsilon}{2 U_D}$$

$$\delta' = \tan \delta \left[\frac{V_o'}{V_o} - \varepsilon' \tan \varepsilon \right] \tag{15}$$

The derivative of ε with respect to x is obtained from equation (5) and is given by the following equation.

$$\varepsilon' = \alpha' + \frac{\cos^2 (\alpha-\varepsilon)}{x-d} [\tan (\alpha-\varepsilon) - \tan \alpha] \tag{16}$$

The derivative of T with respect to α is obtained from equation (6) and is given by the following equation.

$$T' = \frac{x - d}{U_D^2 \, T} [1 + \tan (\alpha-\varepsilon) \tan \alpha] \tag{17}$$

Equations (1 through 5) and (14 through 17) constitute a sufficient set to calculate the jet parameters from a generalized axisymmetric shaped charge once the liner geometry and collapse velocities are known.

2. EXAMINATION OF THE JET PARAMETER EQUATIONS

Before proceeding to a determination of the liner collapse velocity, it is beneficial to evaluate the jet parameter equations in more detail.

Unfortunately, the interdependence of the liner geometry variables and the liner collapse velocities on the collapse angle β do not permit the determination of a unique shaped charge design for given jet parameters. As a result, an initial liner geometry is chosen and a number of calculational iterations are made to determine the required final geometry and/or required collapse velocities. To reduce some of the preliminary

iterations, the dependence of the collapse β on the basic shaped charge variables have been plotted in the following figures.

The variation of the ratio of jet velocity to liner collapse velocity versus β is shown in Figure 2 as a function of $\alpha + \delta$. Figure 3 shows the variation of β with V'_o/V_o as a function of α and r_ℓ for fixed values of $V_o = 0.25$, $\delta = 10^o$, $\delta' = 0$, $\alpha' = 0$, and $T' = 1.5$. For most shaped charges of interest, δ varies from 5° to 15°, δ' is small, α' is zero for a constant angle liner, and T' is approximately 1.5. Thus, this figure provides a good approximation for a constant angle liner geometry and can be useful in selecting the liner angle. As the liner radius increases, the collapse angle β becomes more sensitive to the velocity gradient along the liner. This implies that for a nonconstant collapse velocity, the uncertainties in the jet parameters become greater with increasing liner radius when α is constant. It is also noted that if the collapse velocity is constant along the liner, then the collapse angle is also constant. The slope of the lines shown in Figure 3 are equal for all collapse velocities with only a change in position along the $V'_o/V_o = 0$ coordinate. The variation of β with V_o and α for $V'_o/V_o = 0$ is shown in Figure 4. The combined use of Figures 3 and 4 will yield additional Figure 3's for other collapse velocities.

The use of shaped charge liners with a variable α provides both more flexibility and complexity to the problem. Figure 5 shows the variation of β with α' for other selected parameters. It is interesting to note from this figure that for $\alpha' > 3$, β is nearly independent of V_o'/V_o and r_ℓ. and approaches the values given in Figure 4. It therefore appears that a liner with a variable α will provide a more reproducible jet as well as more flexibility in the design.

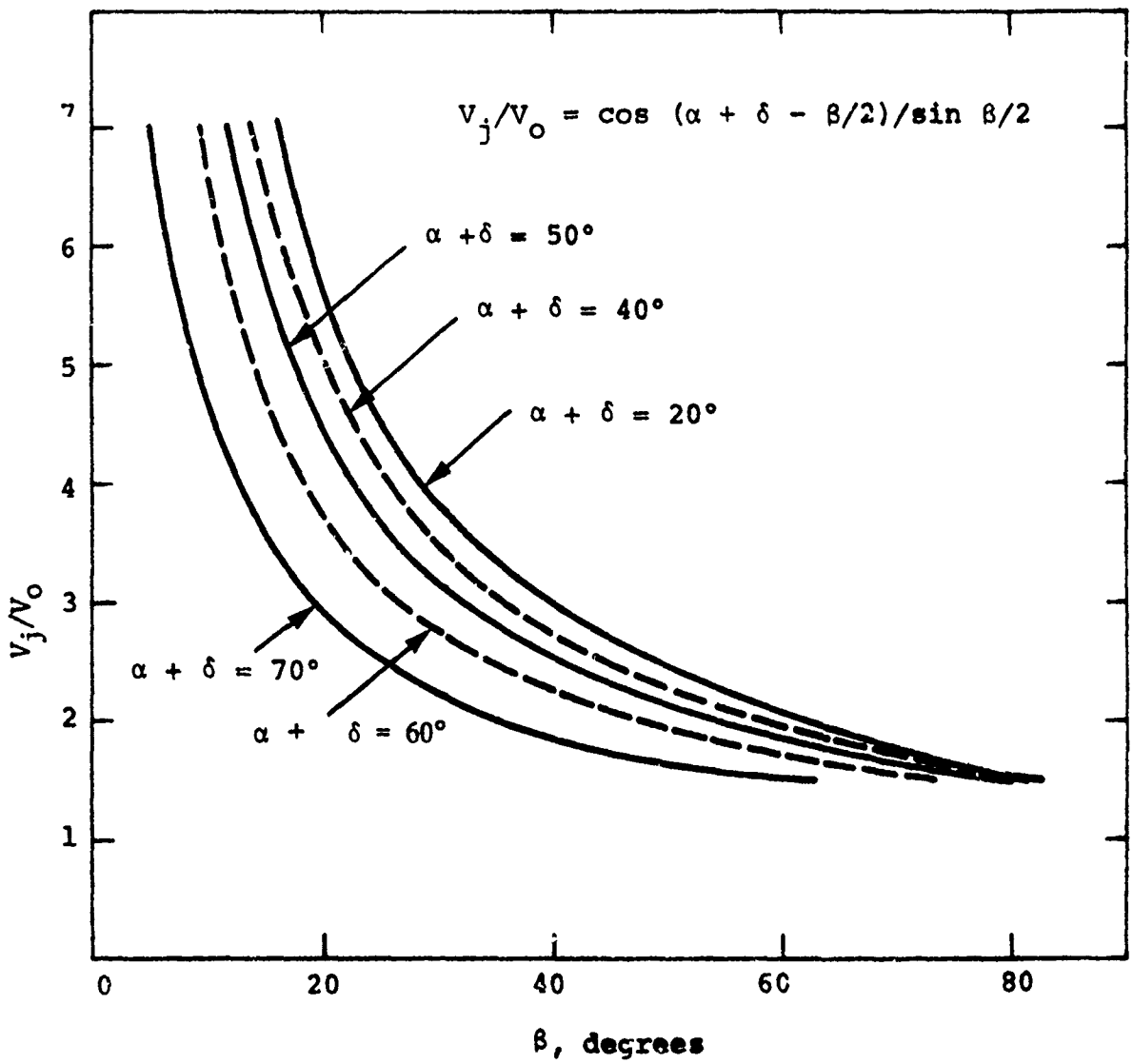

Figure 2. Variation of Jet/Liner Velocity Ratio with β

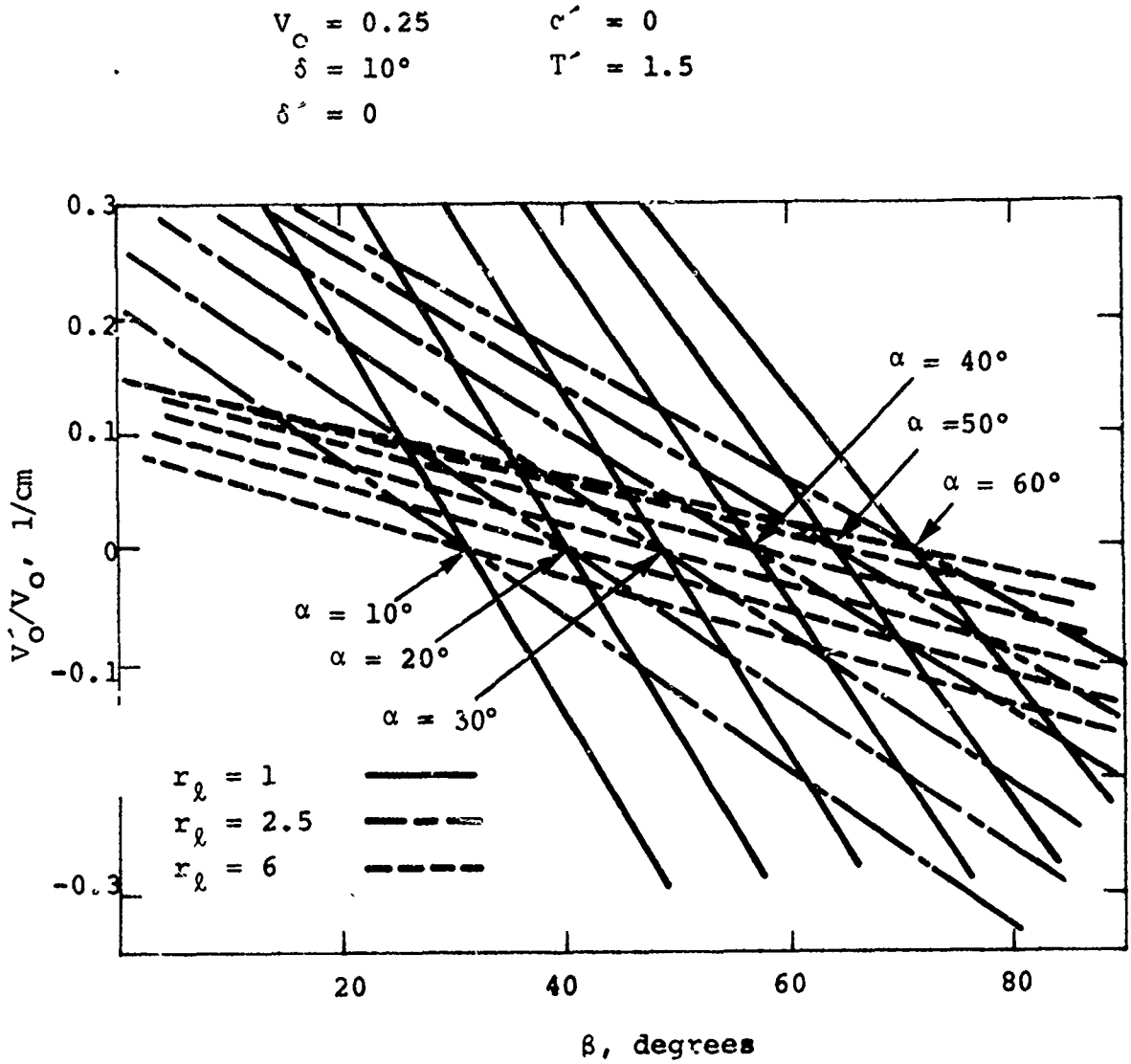

Figure 3. Variation of β with V_o'/V_o

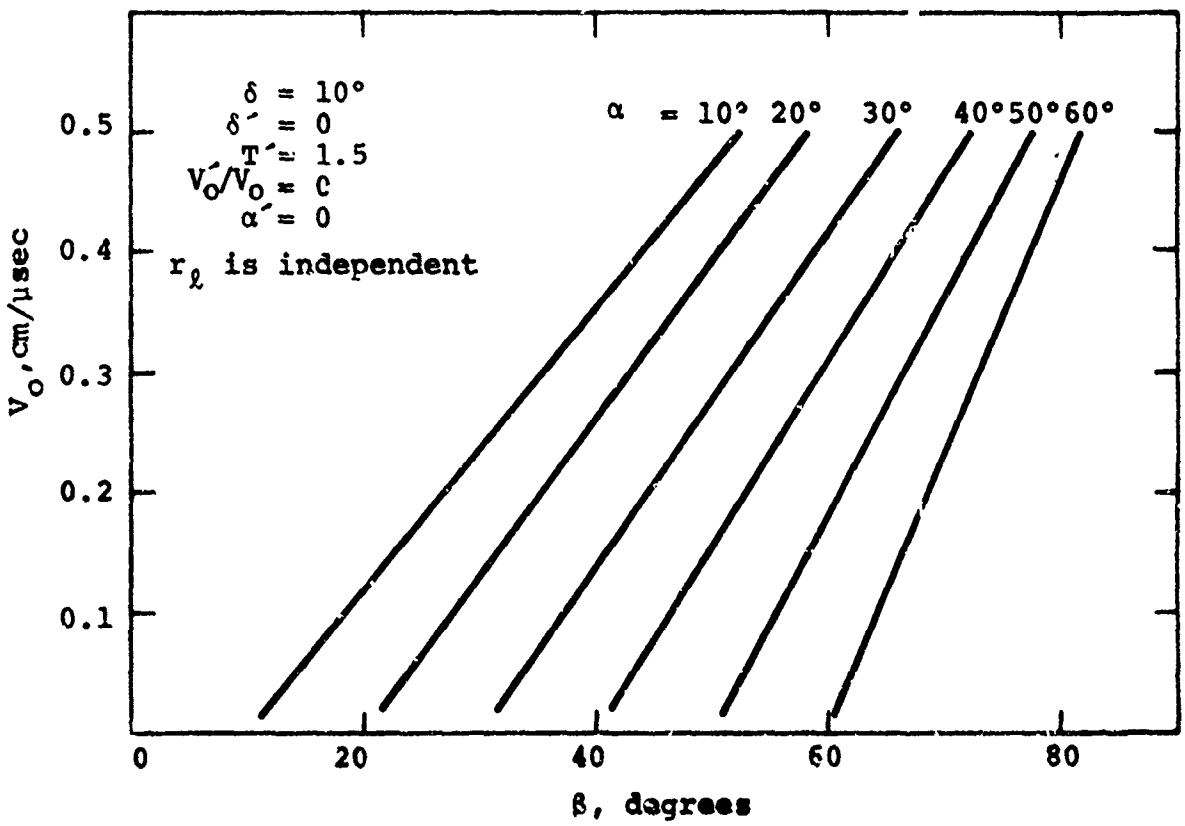

Figure 4. Variation of β with V_o

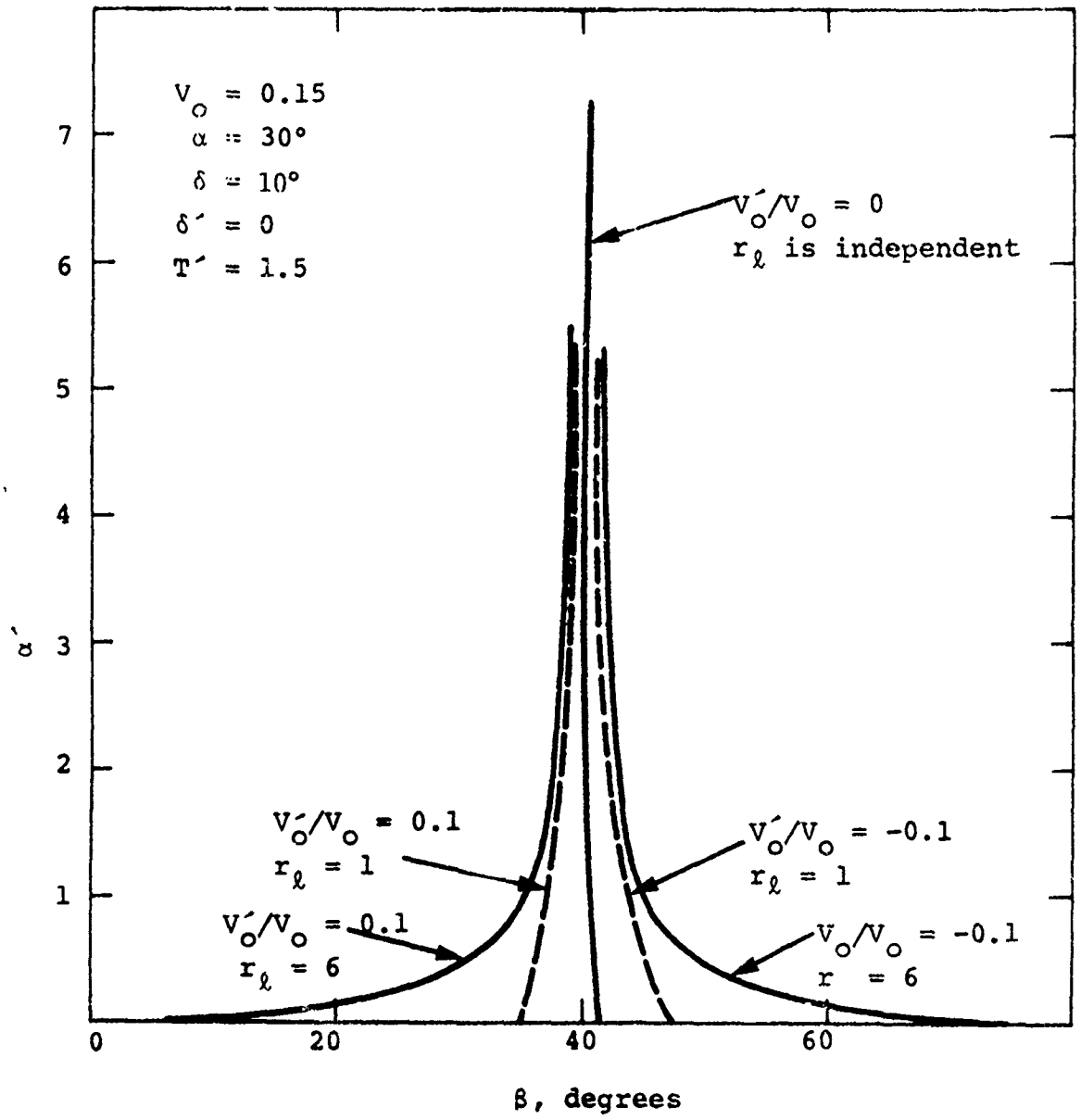

Figure 5. Variation of β with α′

SECTION III

DETERMINATION OF LINER COLLAPSE VELOCITIES

The previous analytical jet parameter equations assumed that the shaped-charge liner could have a variable collapse velocity along its length but not through its thickness. The last part of this assumption implies that the stresses within the liner are small. This is far from true and in fact both the velocity and stress through the liner thickness may vary by factors of two or more. Therefore, the collapse velocity used in the previous equations must be viewed as an equivalent steady state collapse velocity which may or may not be correlated with the actual collapse velocity profile through the liner thickness. The usefulness of the analytical jet parameter equations is then dependent upon the availability of steady state collapse velocity data for imploding cones or cylinders for a variety of liner masses, internal radii, charge mass, etc. Since an extensive experimental and analytical program (References 6 to 9) was required to obtain these data for the 105 mm unconfined shaped charge, it is impractical to obtain the required data in the same manner.

The approach taken in this report to obtain the equivalent steady state collapse velocity is to utilize the existing 105 mm unconfined shaped charge experimental data with one-dimensional calculations of the explosive implosion of cylinders.

1. Approach

Over the past nine years, the contractor has been utilizing linear explosive drivers (References 10 to 13)

to launch projectiles to hypervelocity, simulate nuclear blast waves, drive high performance shock tubes, plus other applications. The linear explosive driver is simply a nonjetting cylindrical shaped charge. As a result of the extensive and variable use of these drivers, the contractor has calculated the collapse process with two-dimensional finite difference continuum mechanics codes, approximated the collapse with one-dimensional codes, and used flash X-ray photography to experimentally determine the collapse geometry. On the basis of this work, it has been found that segments of a conical imploded system can be assumed to act as an equivalent infinite cylinder in a similar geometry. On the basis of this assumption, one-dimensional finite difference calculations were performed which simulated different segments of the 105 mm unconfined shaped charge for which semi-empirical collapse velocity data exists. From a comparison of the calculated velocity history with the data, it was hoped a correlation could be obtained that would allow a determination of the equivalent steady state collapse velocity from additional one-dimensional calculations.

2. Procedure

The BRL 105 mm unconfined shaped charge (Figure 6) was used as the standard for correlation with the one-dimensional cylindrical implosion calculations. The copper liner was then approximated as independent cylindrical segments, driven by a volume burned composition B explosive. The volume burn code option sets the initial pressure in each HE zone equal to one-half the Chapman-Jouquet pressure which has been found to correlate well with experiment. A possible explanation for this correlation is that in a sideward burn the kinetic energy in the detonation products behind the burn front does not participate in the implosion of the cylinder and thus only one-half of the HE energy is available. One-dimensional calculations were

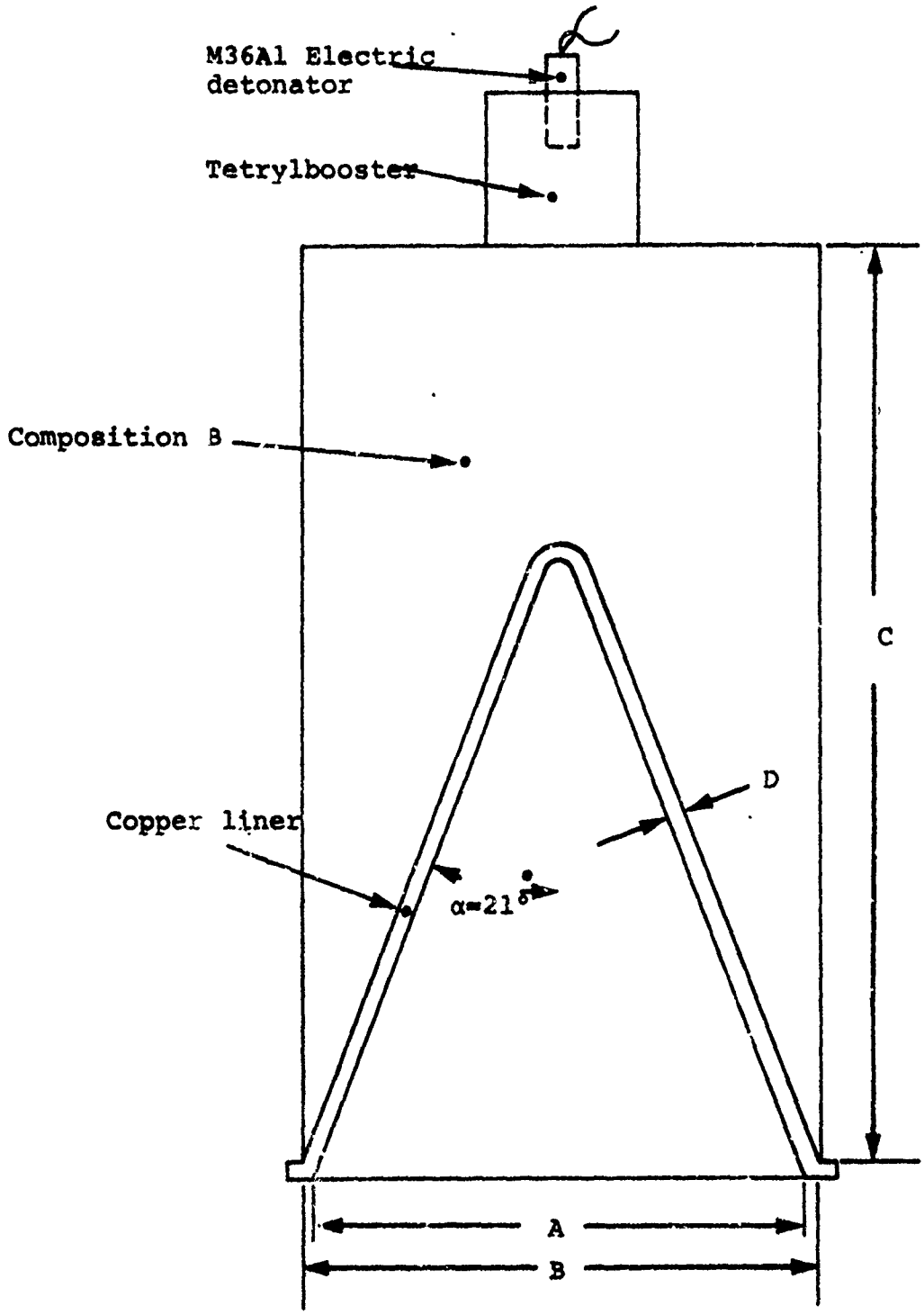

Figure 6. 105mm Unconfined Test Charge. Dimensions are: A = 3.25 in., B = 3.40 in., C = 6 in., and D = 0.106 in.

then run for eleven cylindrical segments at approximately 0.5 cm intervals along the axis ranging from 4 cm to 8.85 cm from the cone apex. The copper liner was divided into fifteen equal radial zones and the velocity and kinetic energy of each zone versus time were monitored. An example of the velocity time profiles at several axial locations are given in Figures 7 to 14.

A review of Figures 7 to 14 shows a number of important phenomena. First, the acceleration of the liner is discontinuous in time as well as variable through the liner thickness. The regions of constant velocity, or zero acceleration, correspond to the round trip transit time of the shock between the point within the liner and either the outside or inside surface of the liner. The effect of the radial convergence of the liner is seen as a rapid increase in the velocity of the inside of the liner just prior to complete collapse. As the liner radius is increased, the velocity gradient through the liner at the time of collapse is reduced. This results from both the reduction in the amount of HE driving the liner with increasing radius as well as more time for the stresses within the liner to equilibrate. It is interesting to note that at 7 μsec, the liner has between 86 and 94 percent of its total kinetic energy.

Since the liner collapse process is very nonsteady, the choice of an equivalent steady state velocity to use in the jet parameter equations will be somewhat arbitrary. The assumption is made that the liner has collapsed at the time the velocity of the second zone has reached a maximum. The time of collapse of the first zone is not used because the zone size of the inside zone will limit the code accuracy during the final convergence and collapse on the axis. Figure 15 shows the velocity profile through the liner at the time of collapse at various points along the liner. Also shown are the semi-empirical

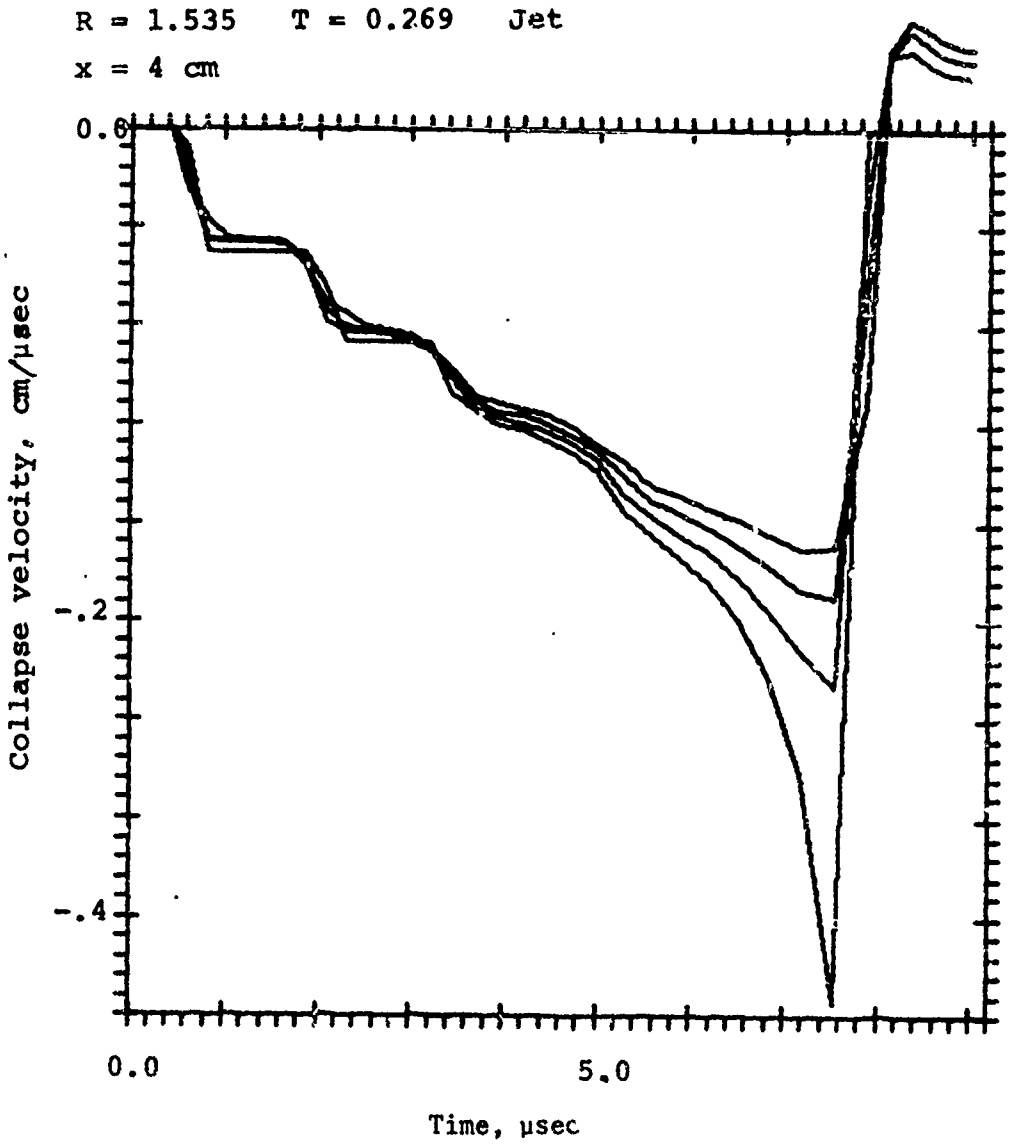

VEL VS TIME AT ZONE NUMBER 0, ORIGINAL POS = 1.27
VEL VS TIME AT ZONE NUMBER 1, ORIGINAL POS = 1.28
VEL VS TIME AT ZONE NUMBER 2, ORIGINAL POS = 1.30
VEL VS TIME AT ZONE NUMBER 3, ORIGINAL POS = 1.32

Figure 7. Collapse Velocity Versus Time at R = 1.535 cm
(Zones 0 through 3)

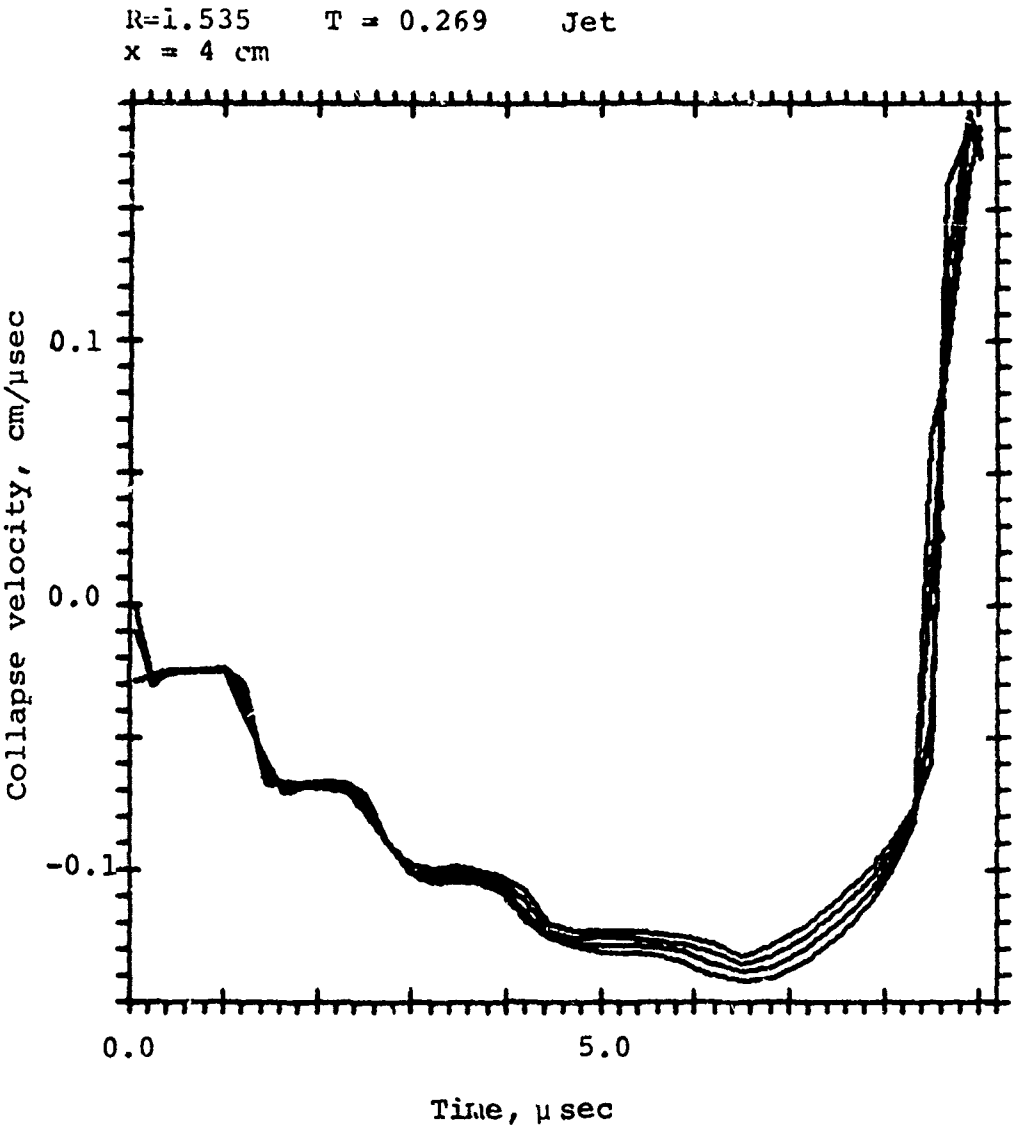

VEL VS TIME AT ZONE NUMBER 12, ORIGINAL POS = 1.48
VEL VS TIME AT ZONE NUMBER 13, ORIGINAL POS = 1.50
VEL VS TIME AT ZONE NUMBER 14, ORIGINAL POS = 1.52
VEL VS TIME AT ZONE NUMBER 15, ORIGINAL POS = 1.53

Figure 8. Collapse Velocity Versus Time at R = 1.535 cm
(Zones 12 through 15)

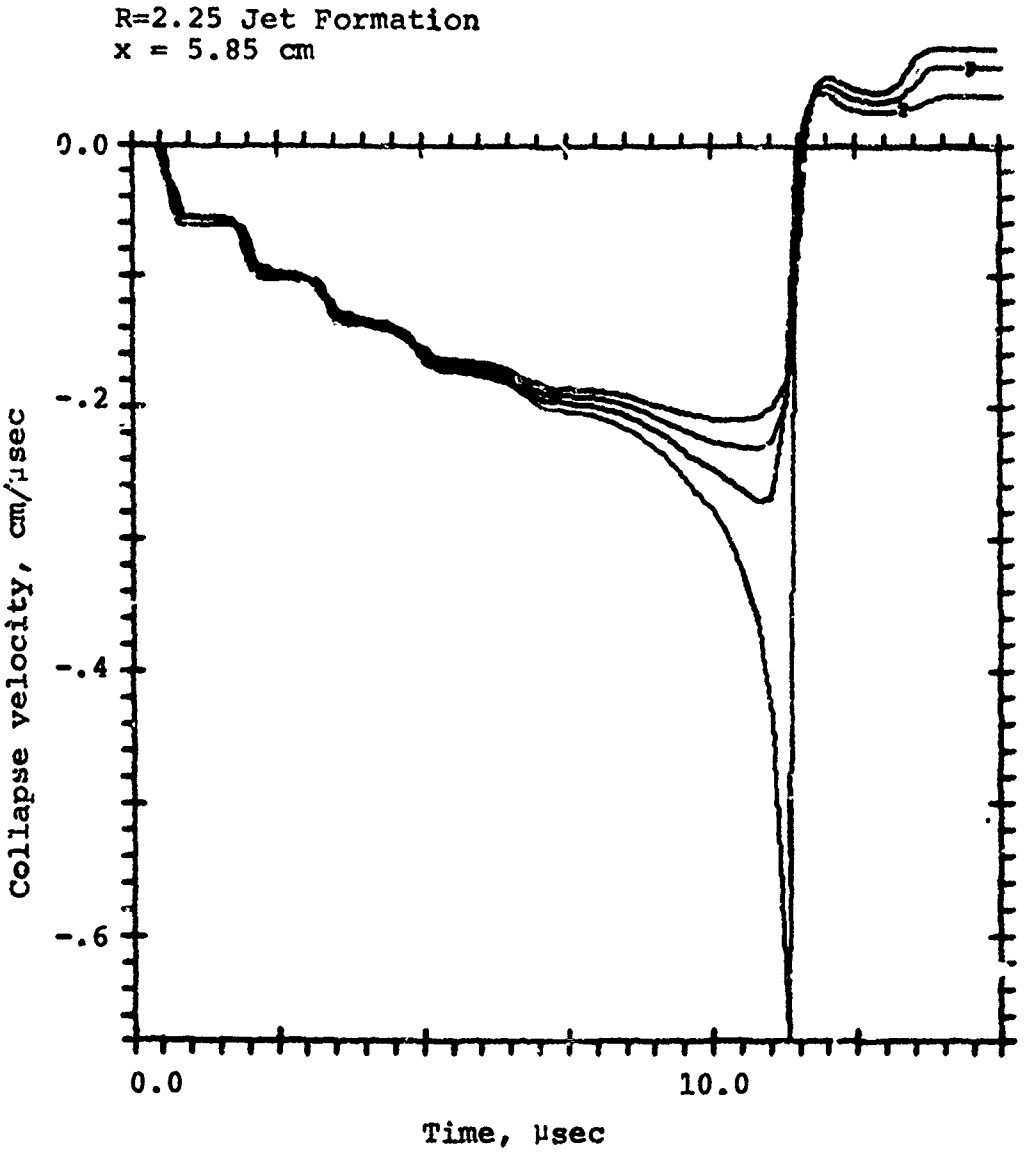

VEL VS TIME AT ZONE NUMBER 0, ORIGINAL POS = 1.98
VEL VS TIME AT ZONE NUMBER 1, ORIGINAL POS = 2.00
VEL VS TIME AT ZONE NUMBER 2, ORIGINAL POS = 2.02
VEL VS TIME AT ZONE NUMBER 3, ORIGINAL POS = 2.03

Figure 9. Collapse Velocity Versus Time at R = 2.25 cm
(Zones 0 through 3)

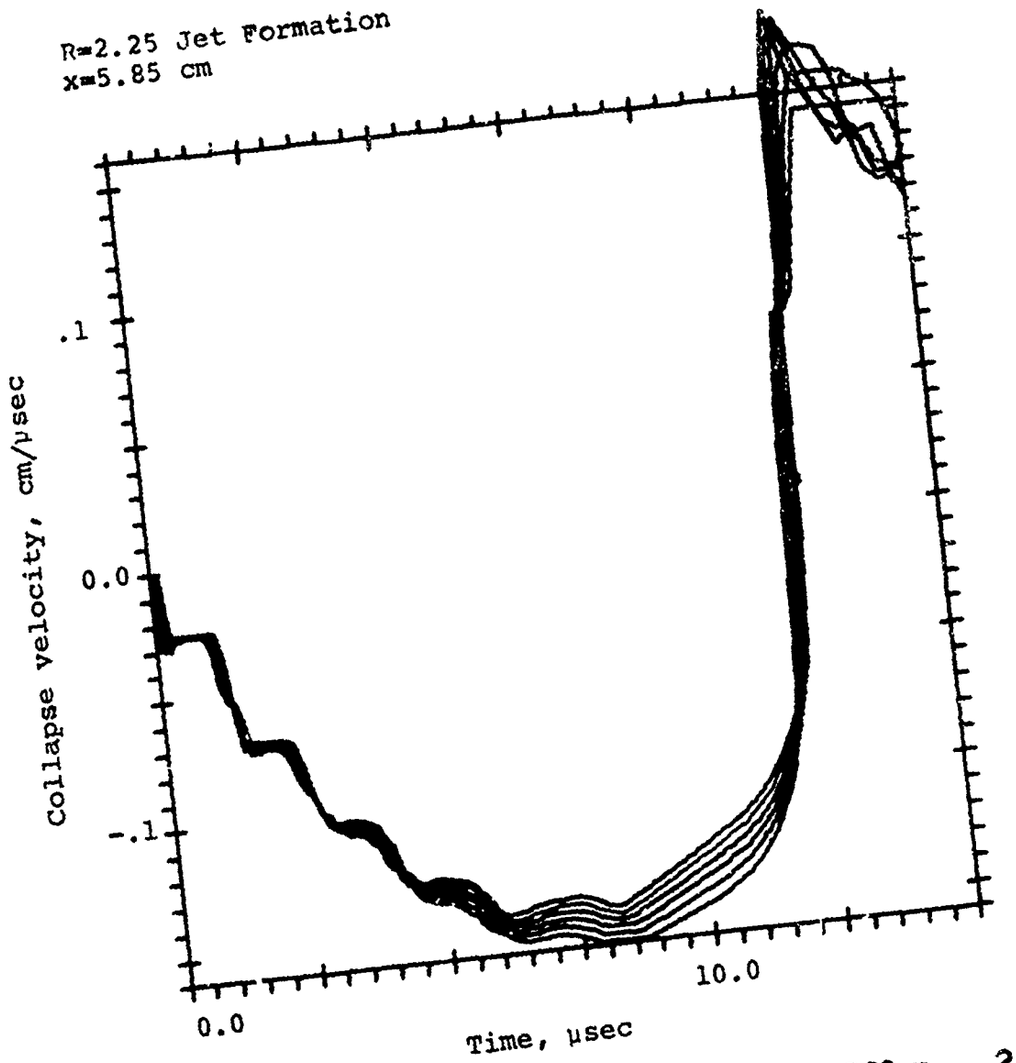

VEL VS TIME AT ZONE NUMBER 10, ORIGINAL POS = 2.16
VEL VS TIME AT ZONE NUMBER 11, ORIGINAL POS = 2.18
VEL VS TIME AT ZONE NUMBER 12, ORIGINAL POS = 2.20
VEL VS TIME AT ZONE NUMBER 13, ORIGINAL POS = 2.21
VEL VS TIME AT ZONE NUMBER 14, ORIGINAL POS = 2.23
VEL VS TIME AT ZONE NUMBER 15, ORIGINAL POS = 2.25

Figure 10. Collapse Velocity Versus Time at R = 2.25 cm (Zones 10 through 15)

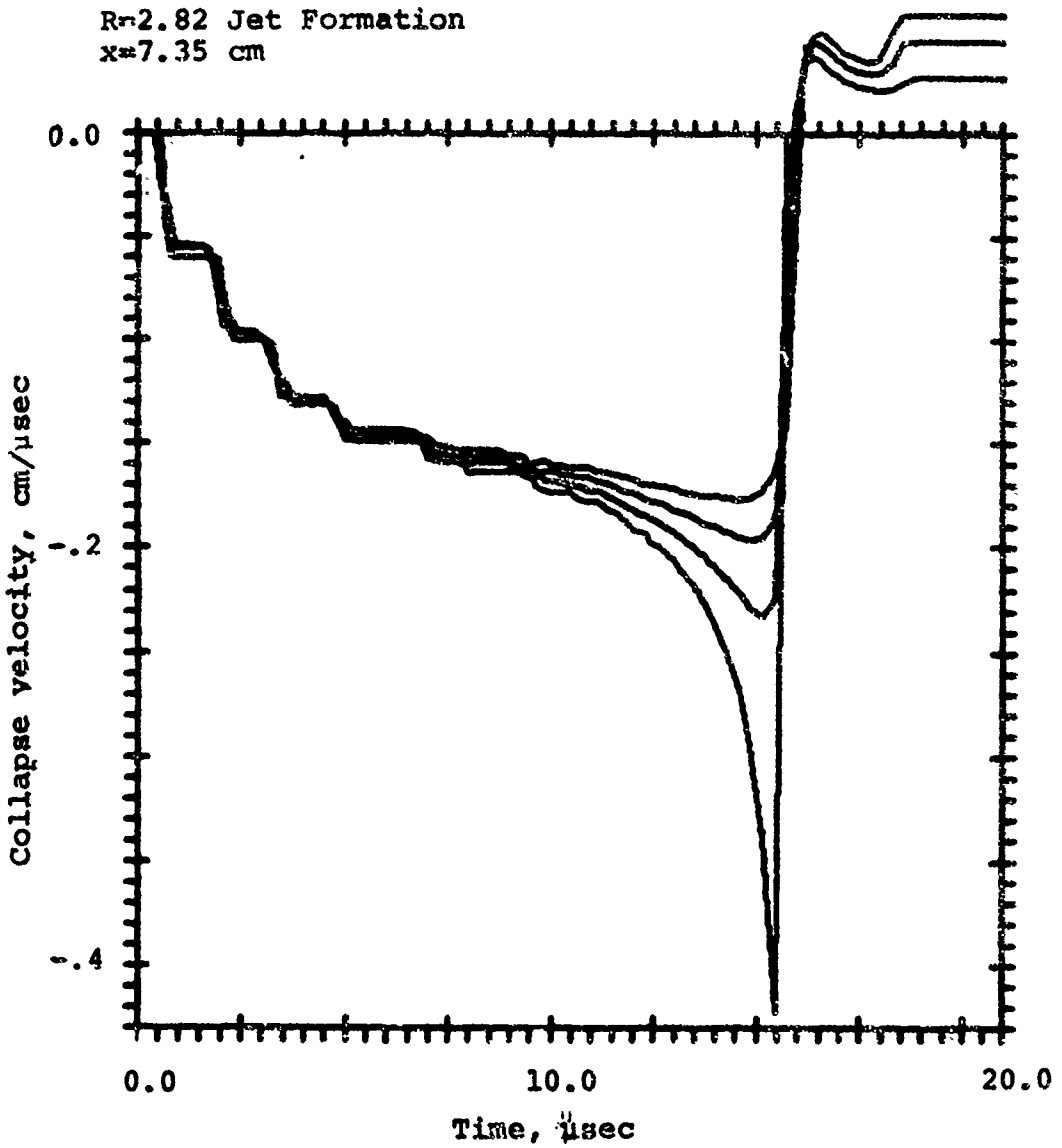

VEL VS TIME AT ZONE NUMBER 0, ORIGINAL POS = 2.55
VEL VS TIME AT ZONE NUMBER 1, ORIGINAL POS = 2.57
VEL VS TIME AT ZONE NUMBER 2, ORIGINAL POS = 2.59
VEL VS TIME AT ZONE NUMBER 3, ORIGINAL POS = 2.60

Figure 11. Collapse Velocity Versus Time at R = 2.82 cm
(Zones 10 through 15)

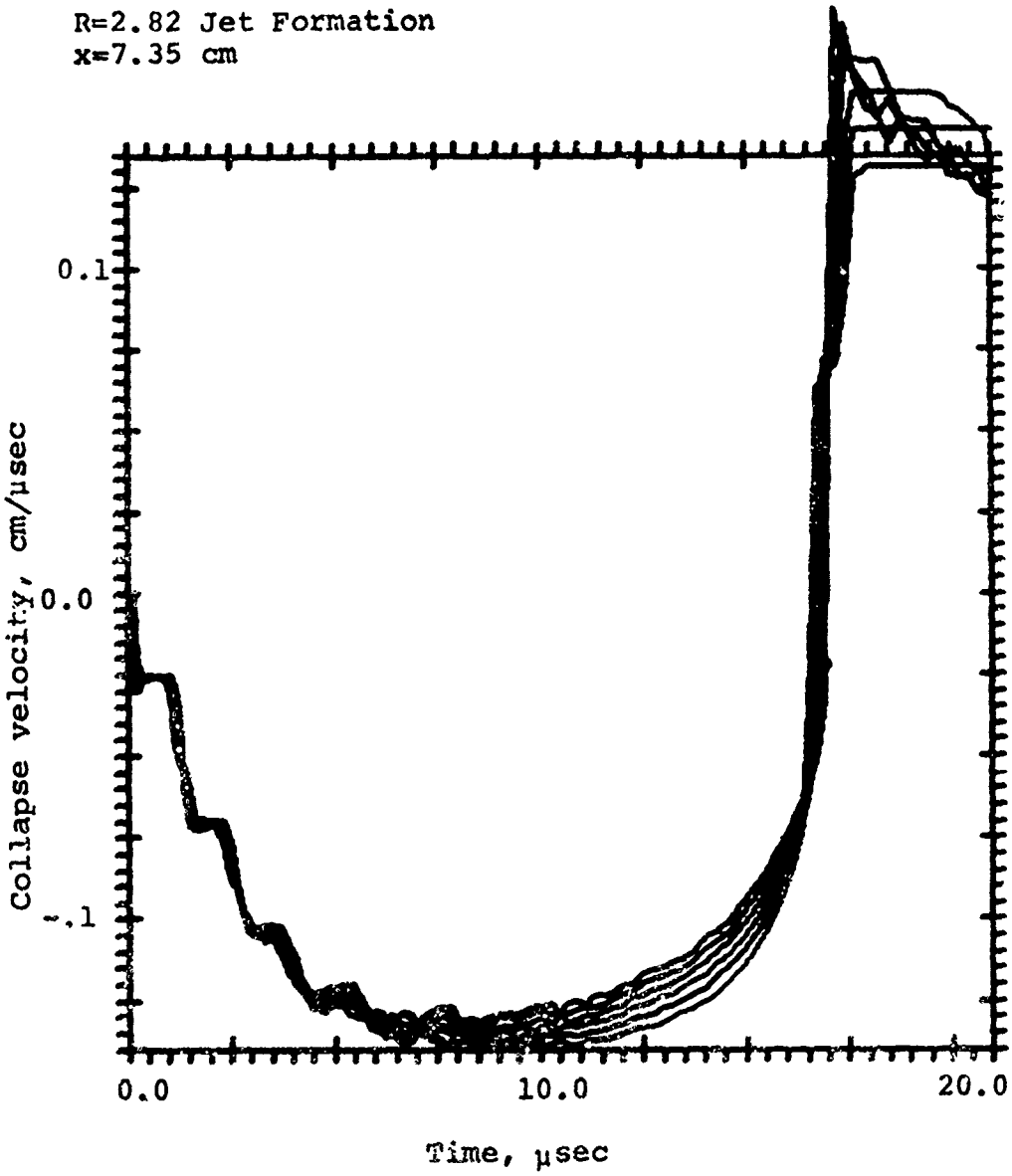

VEL VS TIME AT ZONE NUMBER 10. ORIGINAL POS = 2.73
VEL VS TIME AT ZONE NUMBER 11. ORIGINAL POS = 2.75
VEL VS TIME AT ZONE NUMBER 12. ORIGINAL POS = 2.77
VEL VS TIME AT ZONE NUMBER 13. ORIGINAL POS = 2.78
VEL VS TIME AT ZONE NUMBER 14. ORIGINAL POS = 2.80
VEL VS TIME AT ZONE NUMBER 15. ORIGINAL POS = 2.82

Figure 12. Collapse Velocity Versus Time at R = 2.82 cm
(Zones 10 through 15)

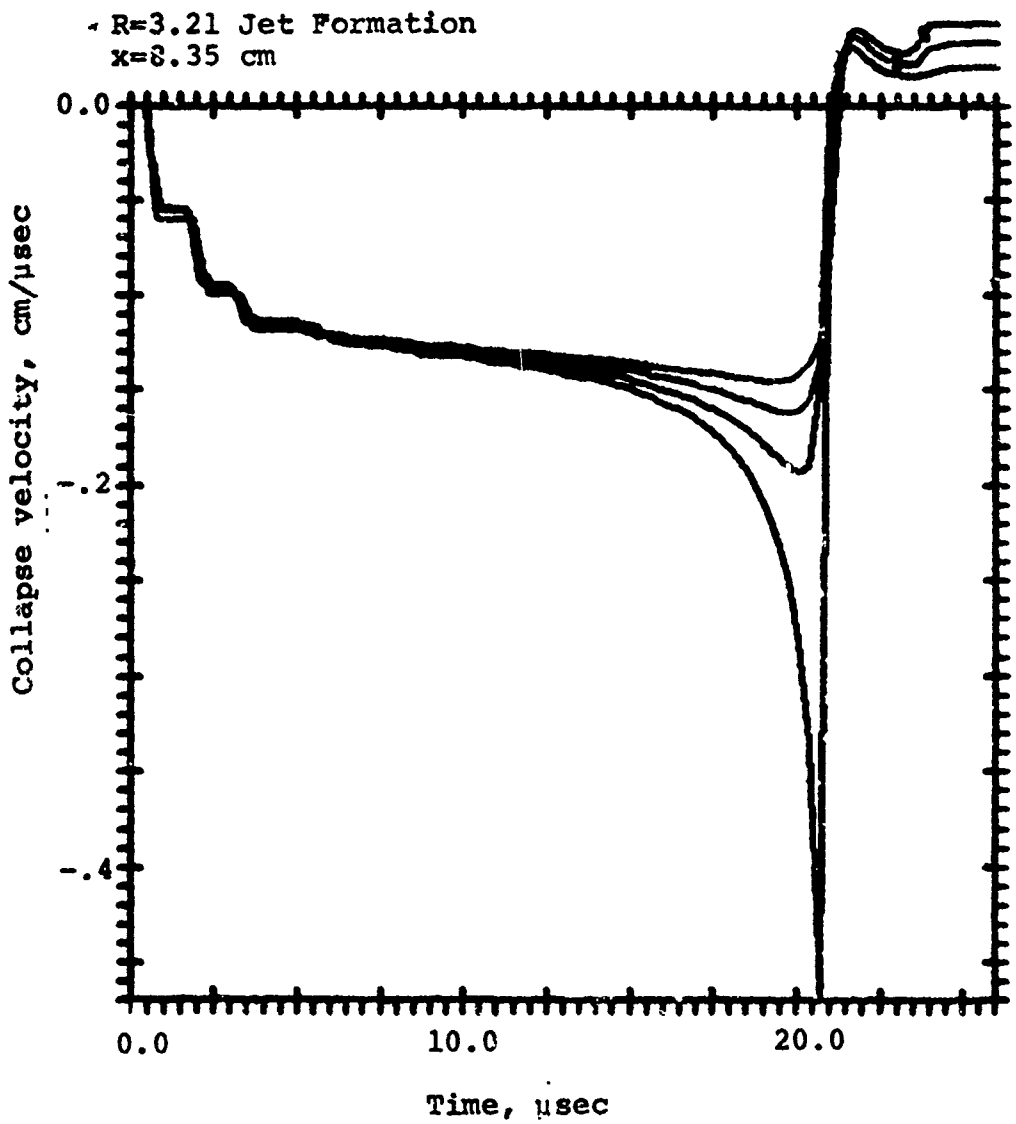

VEL VS TIME AT ZONE NUMBER 0. ORIGINAL POS = 2.94
VEL VS TIME AT ZONE NUMBER 1. ORIGINAL POS = 2.96
VEL VS TIME AT ZONE NUMBER 2. ORIGINAL POS = 2.98
VEL VS TIME AT ZONE NUMBER 3. ORIGINAL POS = 2.99

Figure 13. Collapse Velocity Versus Time at R = 3.21 cm
(Zones 0 through 3)

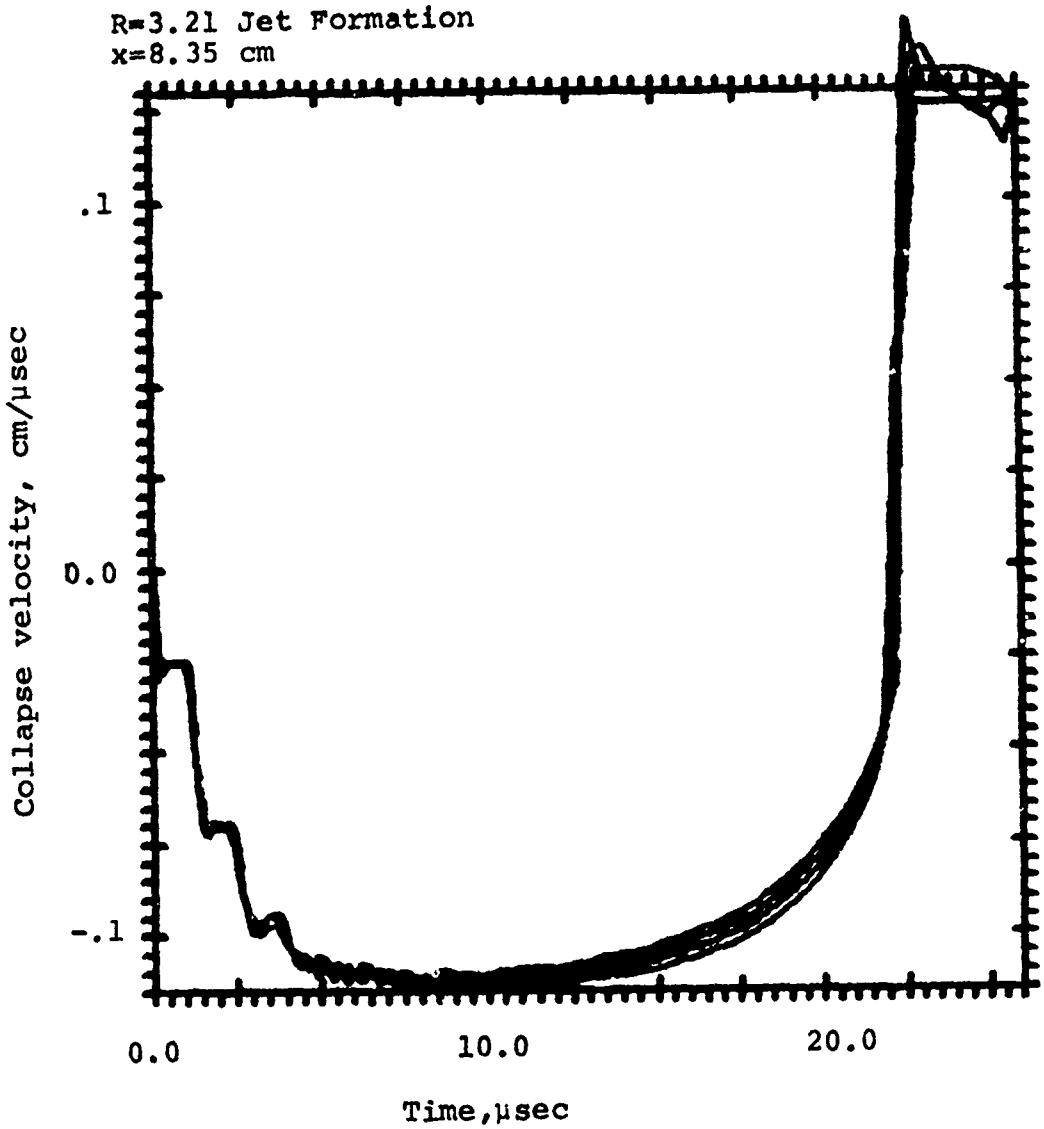

VEL VS TIME AT ZONE NUMBER 12. ORIGINAL POS = 3.16
VEL VS TIME AT ZONE NUMBER 13. ORIGINAL POS = 3.17
VEL VS TIME AT ZONE NUMBER 14. ORIGINAL POS = 3.19
VEL VS TIME AT ZONE NUMBER 15. ORIGINAL POS = 3.21

Figure 14. Collapse Velocity Versus Time at R = 3.21 cm
(Zones 12 through 15)

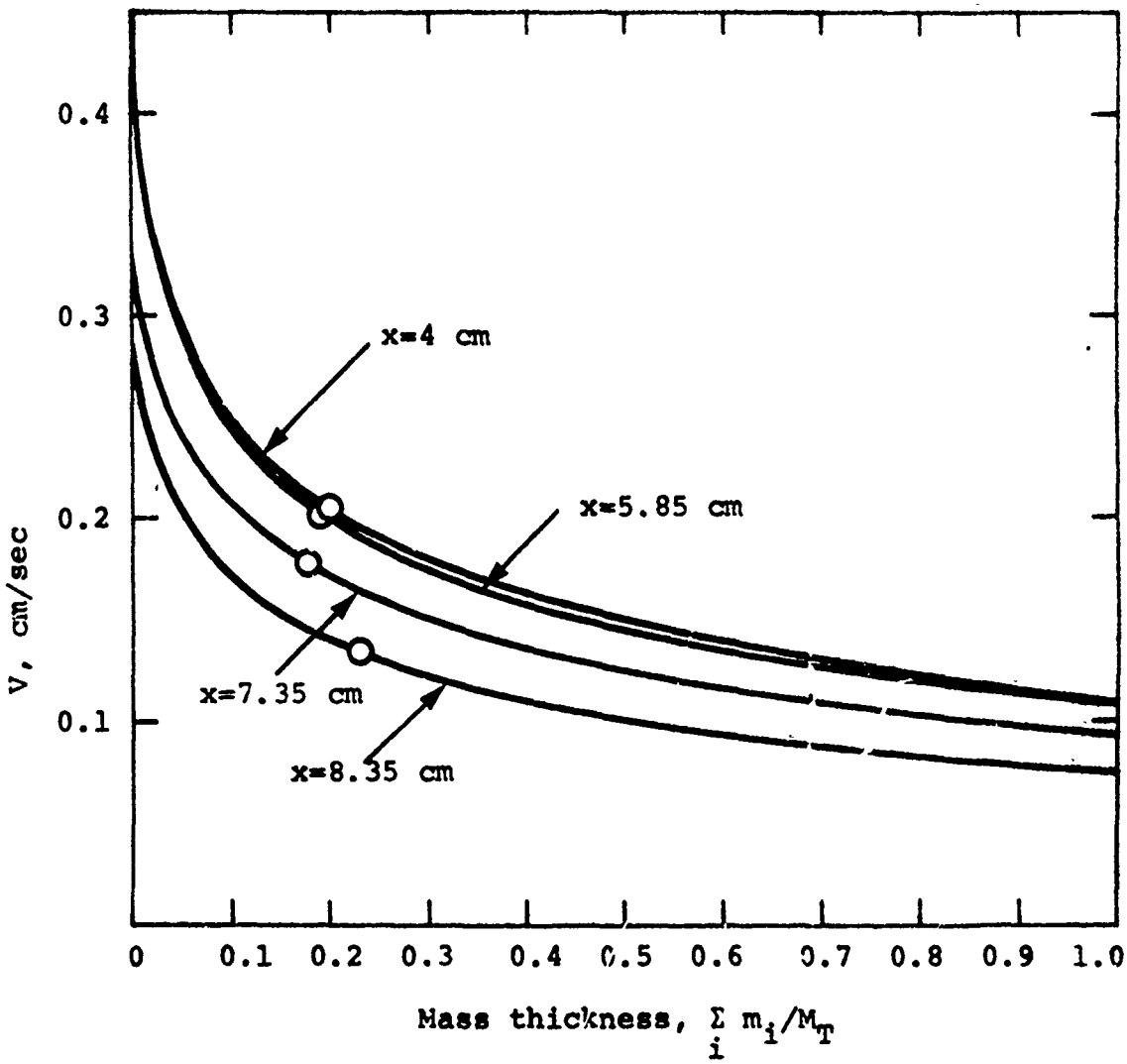

NOTES:

1. 105 mm BRL unconfined shaped charge
2. Zero abscissa is inside radius
3. $\sum_i m_i$ is total mass/length to point i, M_T is total liner mass/length
4. ○ indicates data from 105 mm shaped charge experiments

Figure 15. Velocity Profile Through Liner Thickness at the Time of Collapse

steady state collapse velocity data points from Reference 9. Figure 16 shows the average velocity per increment of the liner. For example, the average velocity of the first 25 percent of the liner is found at the intersection of an ordinate through the abscissa at 0.25 and the appropriate velocity curve. The assumption is now made that either the actual or average velocity of the calculated collapse velocities can be correlated with the steady state data. The form of this assumed correlation is shown in Figure 17. The average velocity correlation was chosen for use because of it being less sensitive to changes in the relative point in the liner thickness and the use of average properties is generally more meaningful than using the actual velocity of some point within the liner.

The curves shown in Figure 17 were plotted as a function of R_i/R_o^* independent of the liner mass. This implies that the location of the equivalent steady state velocity within the liner thickness is primarily dependent upon the internal radius of the liner and the amount of high explosive driving the liner and not on the liner mass. This assumption requires verification. Unfortunately, due to the lack of collapse velocity data, the only way to verify this assumption is by indirect methods. Assuming the two-dimensional finite difference code calculates the jet parameters accurately, then that code can be used to evaluate the above assumption. The alternate method is to calculate the jet parameters of a known shaped charge whose liner mass is considerably larger than the 105 mm unconfined shaped charge.

Using Figure 17 as the key to determine the location within the liner thickness where the calculated average collapse velocity is assumed to be the equivalent steady state collapse velocity, Figure 18 was constructed using the results of 35

---

*R_o is the outside radius at the HE.

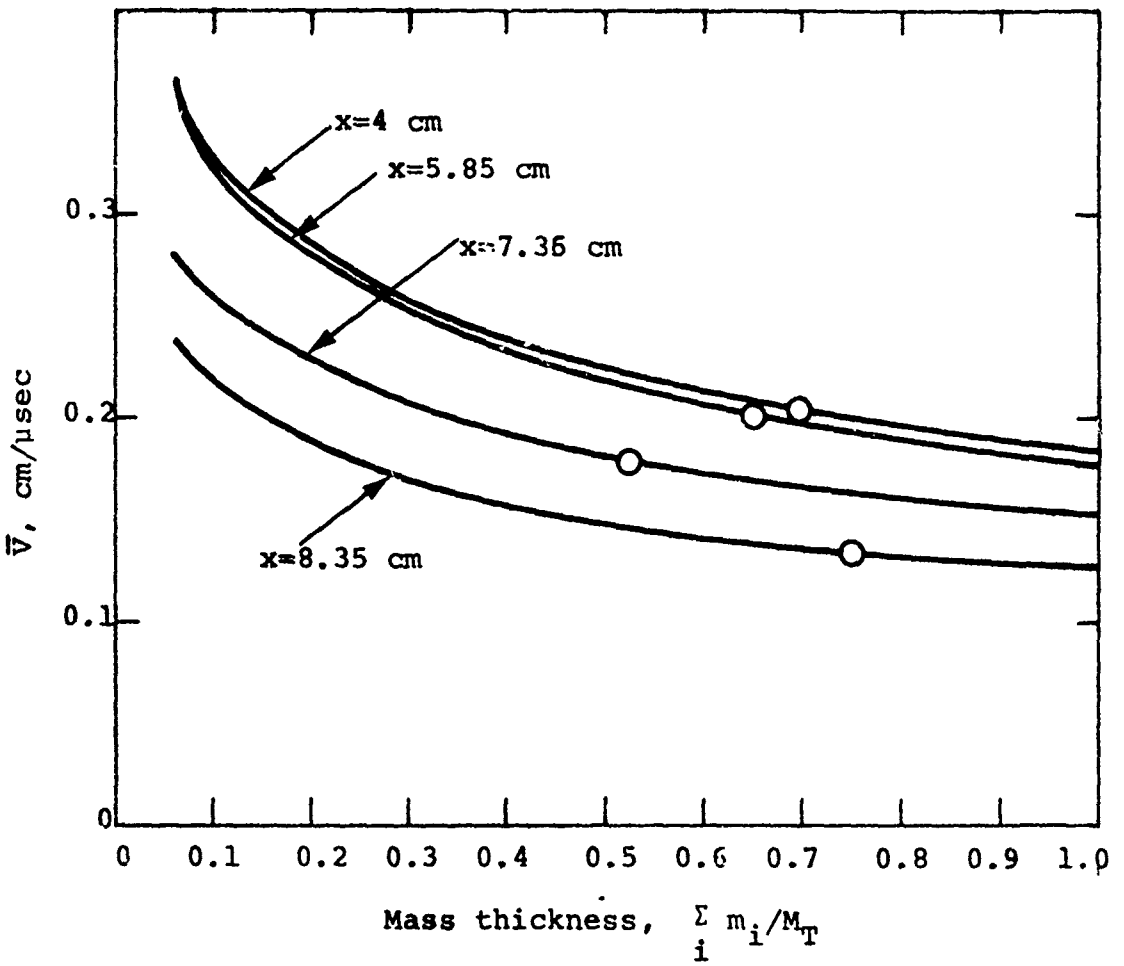

NOTES:

1. 105 mm BRL unconfined chaped charge
2. Zero abscissa is inside radius
3. $\sum_i m_i$ is total mass/length to point i, M_T is total liner mass/length
4. O indicates data from 105 mm shaped charge experiments

Figure 16. Average Velocity Per Liner Increment at the Time of Collapse

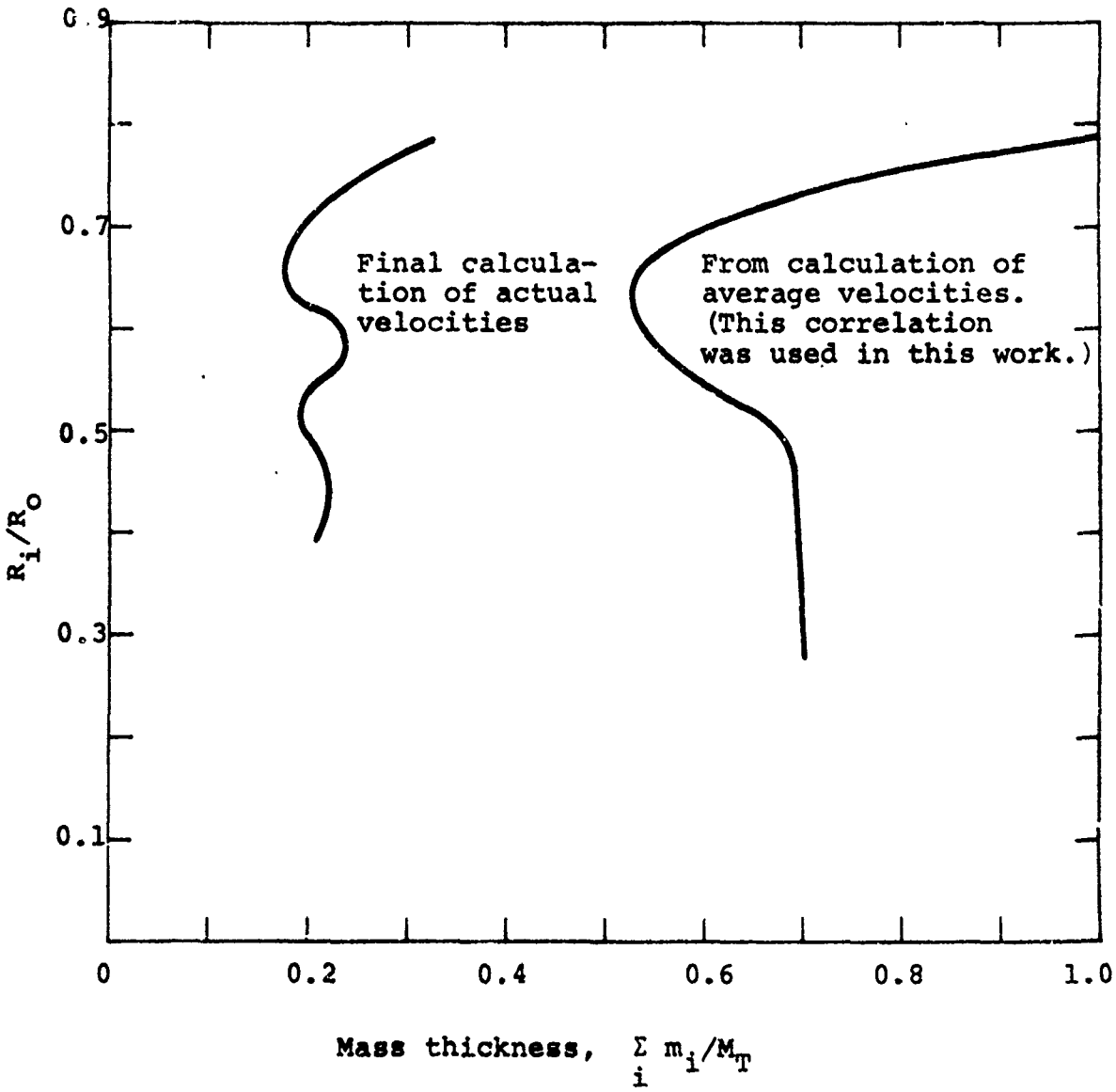

Figure 17. Proposed Correlation Between Calculated and Semi-Empirical Steady State Collapse Velocities

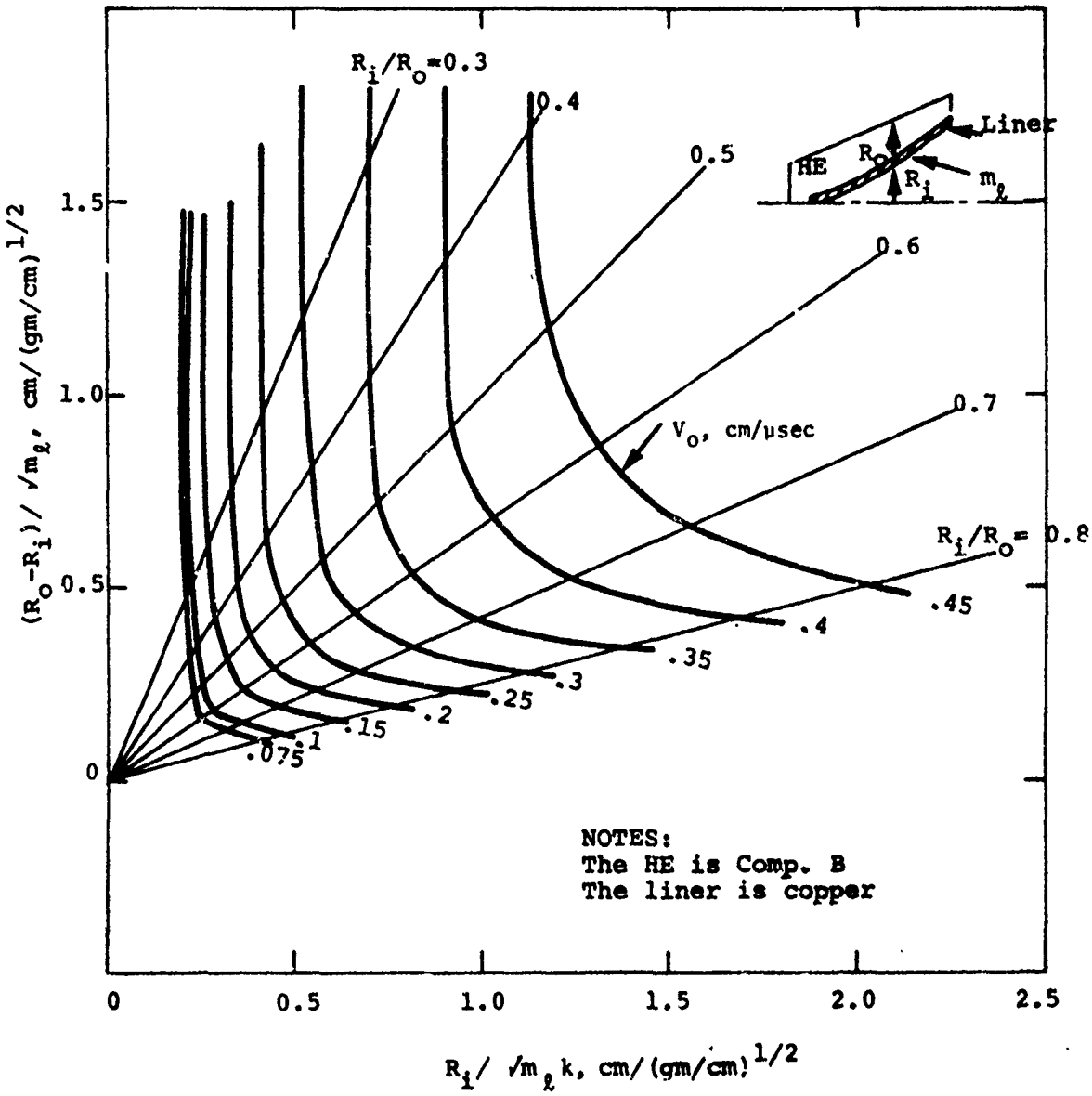

Figure 18. Equivalent Steady State Collapse Velocity For Axisymmetric Imploded Liners

one-dimensional calculations. These calculations used composition B as the high explosive and copper as the liner. To a first approximation, other liner materials may be substituted for copper and the scaling procedure as given in Reference 14 can be used to determine the effect of other explosive loads.

Since the calculated liner collapse velocities are keyed to the empirical data from the 105 mm unconfined shaped charge, the data given in Figure 18 is most accurate for collapse velocities less than 0.25 cm/μsec and for cone angles near 21 degrees. However, for initial design analysis, these curves should suffice.

Figure 18 and the jet parameter equations are sufficient to either calculate the jet parameters from a given shaped charge or to design a shaped charge to give desired jet parameters.

SECTION IV

APPLICATION OF THE JET PARAMETER EQUATIONS

Referring to Figure 18, the effect on the collapse velocity from changing either the HE thickness, the internal liner radius, or the liner mass per unit length is easily seen. For example, increasing the HE thickness such that the ratio of R_i/R_o is decreased below 0.4 does not increase the collapse velocity significantly. On the other hand, increasing the internal radius of the liner such that the ratio R_i/R_o is greater than 0.7 will place unreasonable tolerance limits on the HE thickness to assure a reproducible collapse velocity. Therefore, in terms of good design practice one would probably restrict the geometrical range of interest of R_i/R_o between the limits of 0.4 to 0.7.

1. BRL 105 mm Precision Shaped Charge

Since the finite difference calculation was performed for the BRL 105 mm precision shaped charge, the first example of the use of the jet parameter equations together with Figure 18 also used this same shaped charge. Figure 19 shows the cross section of this shaped charge and Reference 15 discusses the details of its fabrication. The liner of this shaped charge is a remachined liner from a 105 mm unconfined shaped charge. Therefore, the thinner liner of the precision shaped charge with respect to the 105 mm unconfined shaped charge should result in higher liner collapse velocities, higher jet velocities, and smaller jet mass.

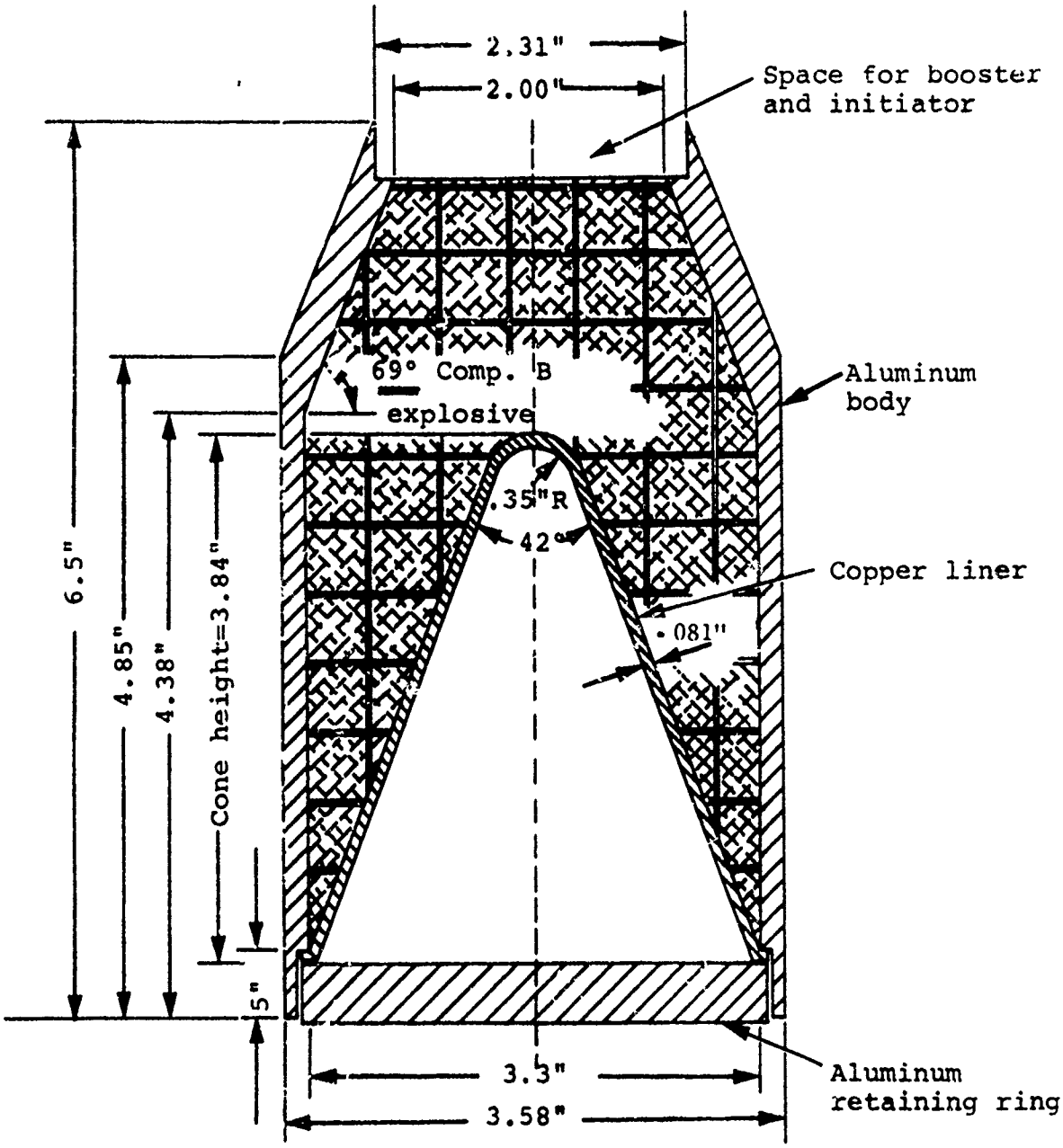

Figure 19. 105mm Precision Shaped Charge Warhead

The liner collapse velocities as a function of axial distance were interpolated from Figure 18 and plotted in Figure 20. The semi-empirical collapse velocities for the 105 mm unconfined shaped charge are also shown in Figure 20 and as anticipated are less than those shown for the precision shaped charge. The smoothed values of the collapse velocity along with its axial derivative were then used in Equation (14) to determine the collapse angle β. The calculated jet velocity and mass are shown in Figure 21 along with data from the 105 mm unconfined shaped charge. As seen, the shape and magnitude of the calculated curves are as expected when compared with the unconfined shaped charge.

2. Design of a Near Constant Jet Velocity Shaped Charge

One possible application of a special designed shaped charge is where large standoff distances are required. For example, conventional shaped charges cannot be used if a 25 foot standoff is required since the jet would have broken up into many ineffective particles before reaching the target. However, if the jet velocities were nearly constant, then the amount of jet elongation and thus time of breakup could be designed to accomplish significant penetration at long standoffs. If a jet could be made that had a constant jet velocity, then only aerodynamic effects would limit its standoff distance. However, since fabrication tolerances will not accommodate such a design, a diverging jet velocity is required to assure sufficient jet length at the target independent of nominal fabrication tolerances. For an illustrative example, consider an initial jet with the following properties:

Initial Jet Length	=	4 cm
Jet Tip Velocity	=	0.58 cm/μsec
Jet Tail Velocity	=	0.54 cm/μsec

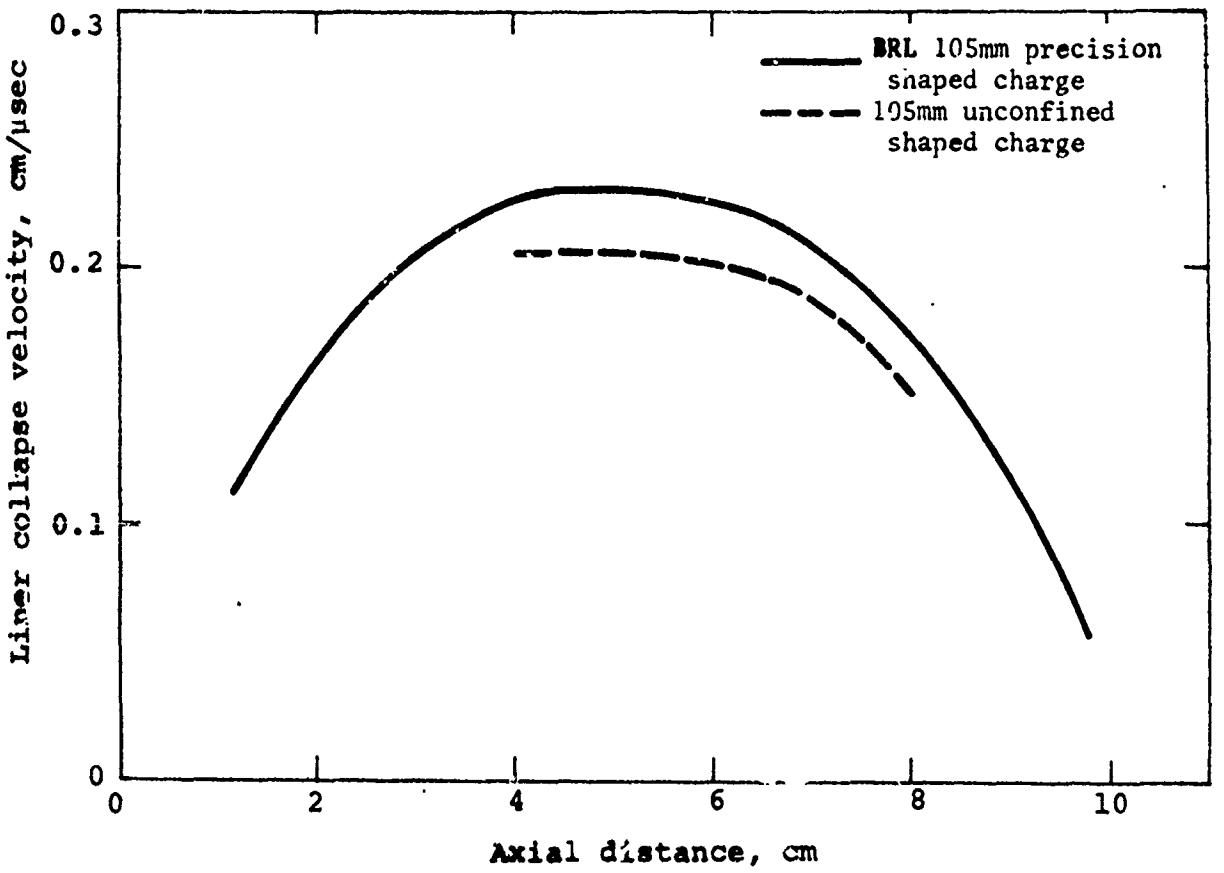

Figure 20. Liner Collapse Velocity for the BRL 105mm Precision Shaped Charge

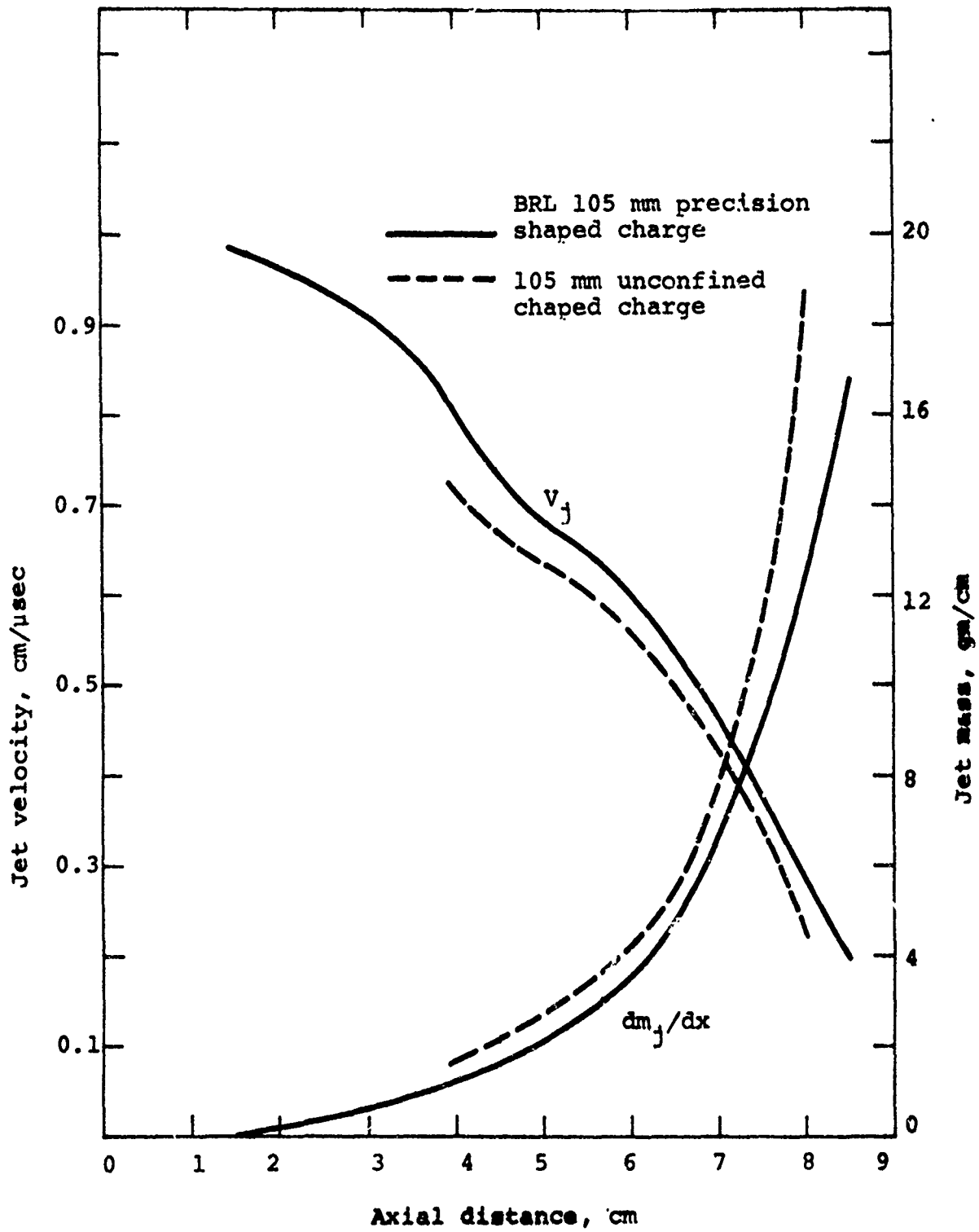

Figure 21. Calculated Jet Parameters for the BRL 105mm Precision Shaped Charge

The tip and tail jet velocities were chosen to (1) stay above any penetration cut-off due to target hardness, (2) account for fabrication tolerances, and (3) limit the jet lengthening to a minimum and maximum of 2 and 25 over a 25-foot distance.*

After iterating on several liner geometries, the one shown in Figure 22 satisfies the above requirements. The procedure used to arrive at Figure 22 was to start with an initial cone angle and collapse velocity to give the jet tip velocity. The cone angle and collapse velocity were then varied incrementally until the desired jet velocity for the next axial segment was obtained. A plot of the resulting liner collapse velocity is shown in Figure 23. Figure 18 was then used to determine the liner mass and high explosive thickness. This last step allows some degree of flexibility in the choice of liner thickness variability and thus jet mass if required. The final jet parameters for this example are given in Figure 24.

*The designed jet lengthening is a factor of 12. The factors of 2 and 25 are for the worst cases of the jet velocities varying by ± 3 percent.

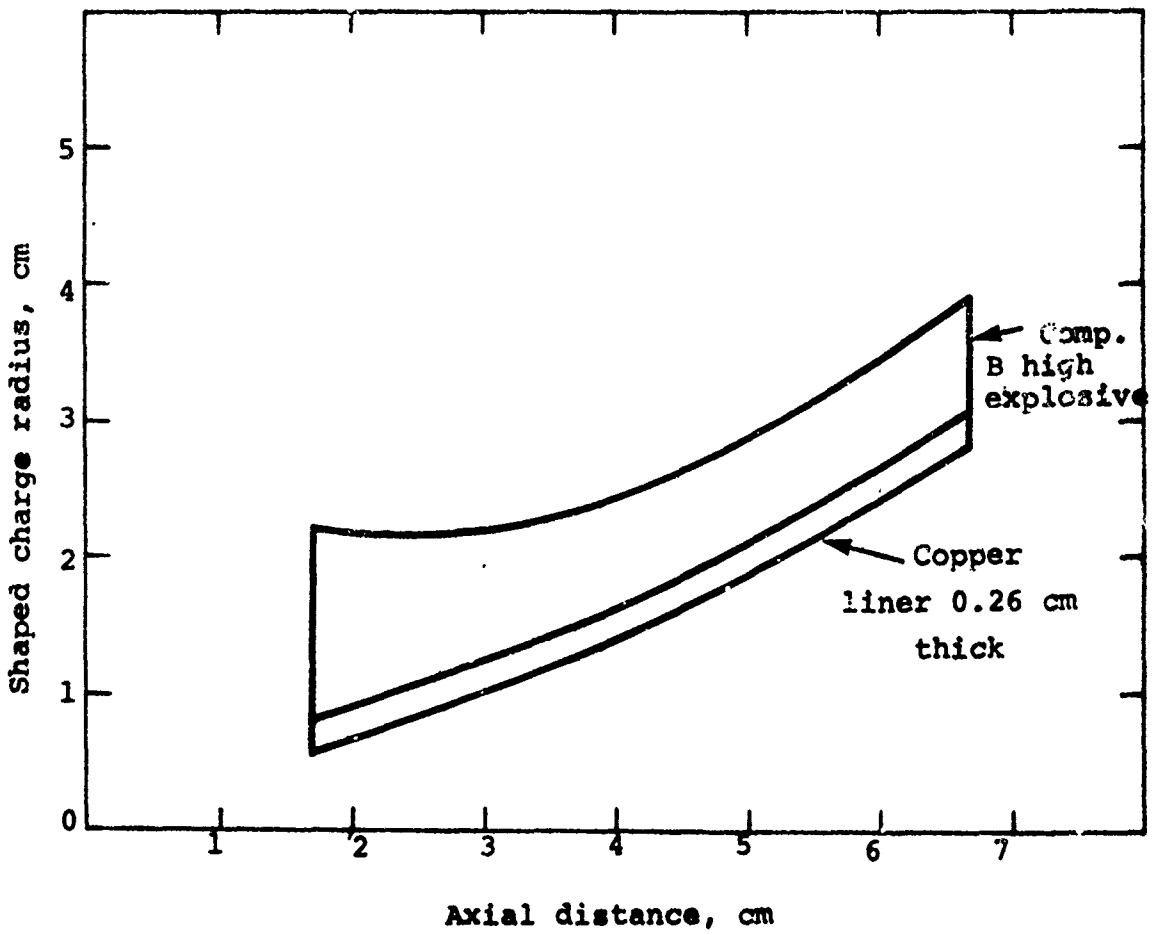

Figure 22. Geometry for a Near Constant Jet Velocity Shaped Charge

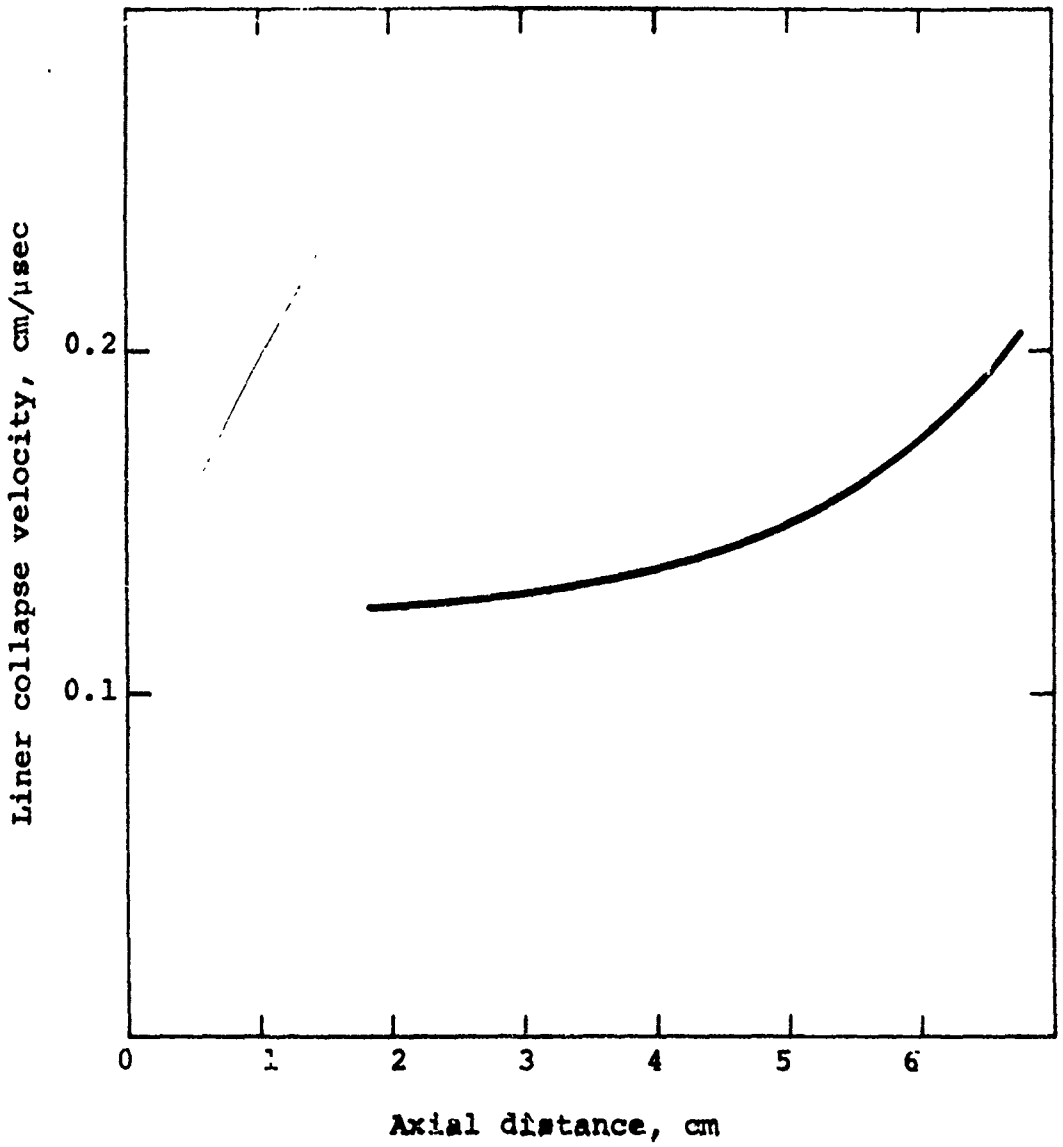

Figure 23. Liner Collapse Velocity for Shaped Charge Geometry Shown in Figure 22

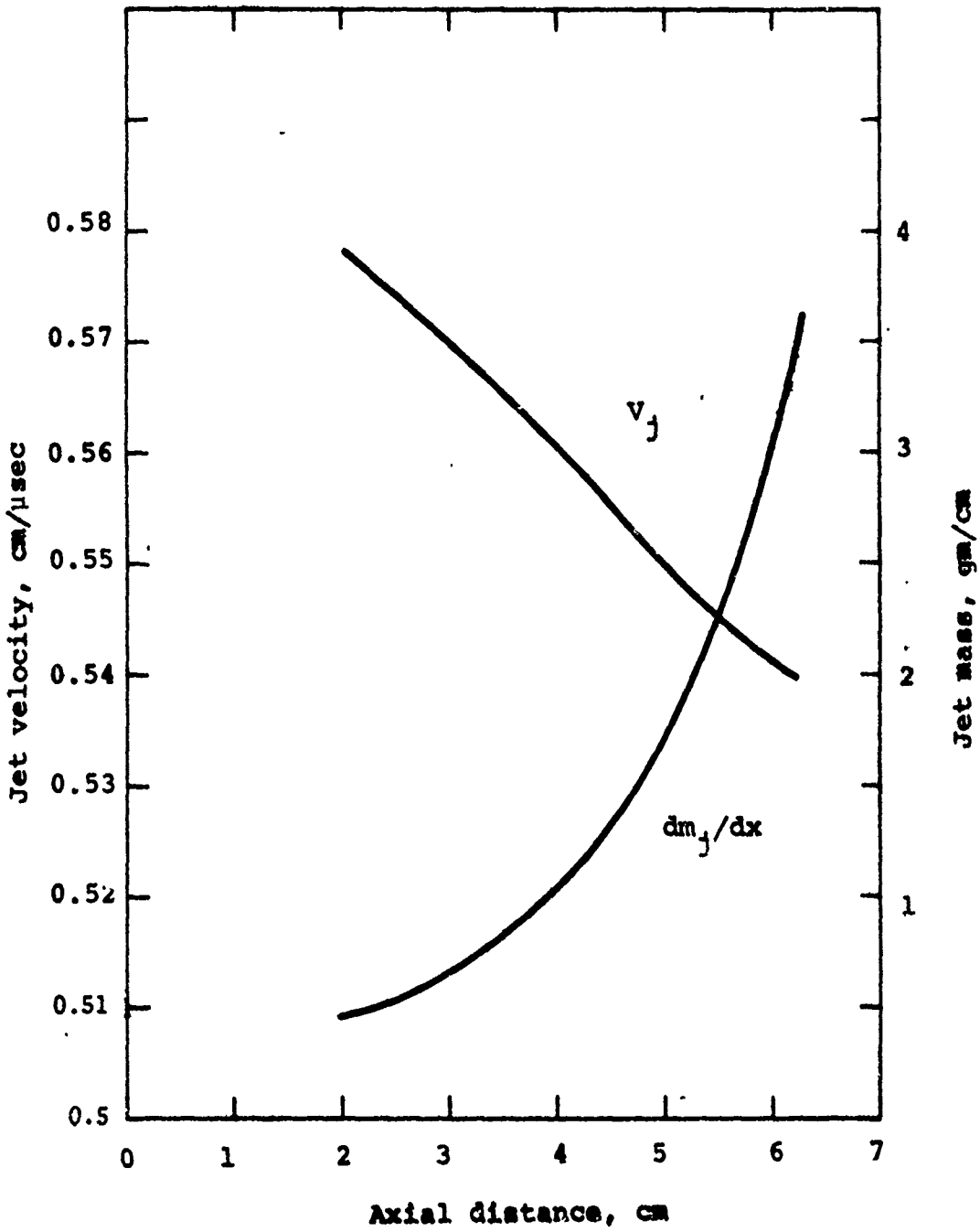

Figure 24. Jet Parameters for Shaped Charge Geometry Shown in Figure 22

SECTION V

CONCLUSION

The nonsteady hydrodynamic theory of jet formation has been extended to include variable geometry liners. In addition, semi-empirical shaped charge collapse data has been combined with one-dimensional cylindrical implosion calculations to obtain liner collapse velocities as a function of explosive thickness, radial distance, and liner mass (Figure 18). The liner collapse velocities given in Figure 18 are the equivalent steady state velocities required in the theory of jet formation.

It is now possible to calculate the jet parameters from existing shaped charges without resorting to the use of two-dimensional calculations or elaborate experiments. More significant, the combined use of the collapse velocity curves plus the jet formation theory provides a basis from which a shaped charge can be designed to give predetermined jet parameters. Thus special warhead applications may be practical or perhaps standard shaped charges can be designed to perform the same task more efficiently. Additionally, the curves can be ed to estimate the variability in the jet parameters from uncertainties in the fabrication process.

Two examples of the use of the jet formation theory combined with the collapse velocity curves from Figure 18 were given in the previous section. To verify the adequacy of this design technique it is suggested that a special shaped-charge warhead be specified, designed, fabricated and tested. To the extent that this design technique can be validated, the design of future shaped-charge warheads can be greatly simplified.

(The reverse of this page is blank)

REFERENCES

1. Birkoff, G., MacDougal, D., Pugh, E., Taylor, G., "Explosives with Lined Cavities," J. Appl. Phys. 19, 563, (1948).

2. Pugh, E., Eichelberger, R., Rostoker, N., "Theory of Jet Formation by Charges with Lined Conical Cavities," J. Appl. Phys. 23, 5, 532 and 537, (1952).

3. Eichelberger, R.,"Re-Examination of the Non-Steady Theory of Jet Formation by Lined Cavity Charges," J. Appl. Phys. 26, 4, 398, (1955).

4. Defourneaux, M., Elementary Theory of Linear Shaped Charges, The Saint-Louis Franco-German Research Institute, Technical Report T44/68, October 1969.

5. Kiwan, A., Wisniewski, H., Theory and Computations of Collapse and Jet Velocities of Metallic Shaped Charge Liners, BRL Report 1620, Nov. 1972.

6. Bryan, G. M., Eichelberger, R. J., MacDonald, D. and Zigman, P. E. "Application of Radioactive Tracers to the Study of Shaped Charge Phenomena," J. Appl. Phys. 28, 1152, (1957).

7. Gainer, M. K. The Application of Radioactive Tracers to Shaped Charge Liners, BRL Memorandum Report No. 1242, January 1960.

8. Feldman, James B., Jr., Volume-Energy Relation from Shaped Charge Jet Penetrations, Proceedings of the Fourth Symposium on Hypervelocity Impact, APGC-TR-60-39 (II), September 1960.

9. Allison, F., Vitali, R., An Application of the Jet Formation Theory to a 105 mm Shaped Charge, BRL Report 1165, March 1962.

10. Watson, J. D., An Explosively Driven Gun to Launch Large Models to Reentry Velocities, PIFR-098, Physics International Company, San Leandro, California, April 1960.

11. Watson, J. D., Moore, E. T., Jr., Mumma, D., Marshall, J. S., Explosively-Driven Light Gas Guns, PIFR-024/065, Physics International Company, San Leandro, California, September 1967.

REFERENCES (concluded)

12. Moore, E. T., Jr., Explosive Hypervelocity Launchers, NASA CR-982, Physics International Company, San Leandro, California, February 1968.

13. Flagg, R. F., Marshall, J. S., Jr., Watson, J. D., Moore, E. T., Jr., Explosively-Driven Launchers, PIPR-098-SA-1, Physics International Company, San Leandro, California, April 1968.

14. Jonas, G., Merendino, A., Prediction of Shaped Charge Jet and Penetration Parameters with Various Explosive Loadings, BRL Memorandum Report No. 1494, July 1963.

15. DiPersio, R., Simon, J., Merendino, A., Penetration of Shaped-Charge Jets into Metallic Targets, BRL Report No. 1296, September 1965.

UNCLASSIFIED

SECURITY CLASSIFICATION OF THIS PAGE (When Data Entered)

REPORT DOCUMENTATION PAGE

READ INSTRUCTIONS BEFORE COMPLETING FORM

1. REPORT NUMBER: AFATL-TR-73-160, Volume I

2. GOVT ACCESSION NO.:

3. RECIPIENT'S CATALOG NUMBER:

4. TITLE (and Subtitle): Calculation of Shaped-Charge Jets Using Engineering Approximations and Finite Difference Computer Codes. Volume I. Generalized Analytical Approach to Shaped-Charge Warhead Design

5. TYPE OF REPORT & PERIOD COVERED: Final Report - June 1972 to April 1973

6. PERFORMING ORG. REPORT NUMBER: PIFR-430

7. AUTHOR(s): L. Behrmann

8. CONTRACT OR GRANT NUMBER(s): F08635-72-C-0229

9. PERFORMING ORGANIZATION NAME AND ADDRESS:
Physics International Company
2700 Merced Street
San Leandro, California 94577

10. PROGRAM ELEMENT, PROJECT, TASK AREA & WORK UNIT NUMBERS:
Project No. 670B
Task No. 10
Work Unit No. 02

11. CONTROLLING OFFICE NAME AND ADDRESS:
Air Force Armament Laboratory
Air Force Systems Command
Eglin Air Force Base, Florida 32542

12. REPORT DATE: August 1973

13. NUMBER OF PAGES: 52

14. MONITORING AGENCY NAME & ADDRESS (if different from Controlling Office):

15. SECURITY CLASS. (of this report):

15a. DECLASSIFICATION/DOWNGRADING SCHEDULE:

16. DISTRIBUTION STATEMENT (of this Report)

Distribution limited to U. S. Government agencies only; this report documents test and evaluation; distribution limitation applied August 1973. Other requests for this document must be referred to the Air Force Armament Laboratory (DLYA), Eglin Air Force Base, Florida 32542.

17. DISTRIBUTION STATEMENT (of the abstract entered in Block 20, if different from Report)

18. SUPPLEMENTARY NOTES

Available in DDC

19. KEY WORDS (Continue on reverse side if necessary and identify by block number)

Shaped-Charge Design Procedure
Jet Penetration Characteristics
Shaped-Charge Launcher
Mechanics of Jet Formation
Non-Steady State Theory of Jet Formation
One-Dimensional Finite Difference Continuum Mechanics Calculations
Two-Dimensional Finite Difference Continuum Mechanics Code
Jet Stability

20. ABSTRACT (Continue on reverse side if necessary and identify by block number)

This report describes a technique to optimize the current shaped charge design procedure as follows. Starting with the desired target to be defeated, a determination of the desired penetration characteristics of the jet would be made. Existing jet penetration theory would then be used to estimate the ideal characteristics of the jet to defeat the given target. A shaped charge launcher would then be designed to give these ideal jet

DD FORM 1 JAN 73 1473 EDITION OF 1 NOV 65 IS OBSOLETE

UNCLASSIFIED

SECURITY CLASSIFICATION OF THIS PAGE (When Data Entered)

characteristics. However, a suitable design procedure requires: (1) a viable analytical or empirical design approach to obtain a first cut shaped charge design, (2) a better understanding than now exists of the detailed mechanisms of jet formation, and (3) a better understanding of the phenomenon of jet penetration. This report, which is contained in two volumes, addresses the first two of these requirements. Volume I describes the use of the existing non-steady state theory of jet formation with experimental data and one-dimensional finite difference continue mechanics calculations to obtain the liner collapse velocity for generalized axisymmetric shaped charges. The results of this work are then used to obtain nonunique shaped charge designs which give the required idealized jet parameters. Volume II describes the modification and utilization of a two-dimensional finite difference continuum mechanics code utilizing the Lagrangian Coordinate system to calculate the complete jet formation parameters for any generalized axisymmetric shaped charge. The utilization of this code allows a more detailed study of such phenomena as jet stability, bifurcation on the axis, shear gradients, viscosity, shocks, incipient vaporization, surface tension, and possible other effects. The combined use of both the engineering formulations along with the sophisticated two-dimensional code calculation allows design engineers the versatility to design the most optimum shaped charge for their particular application.